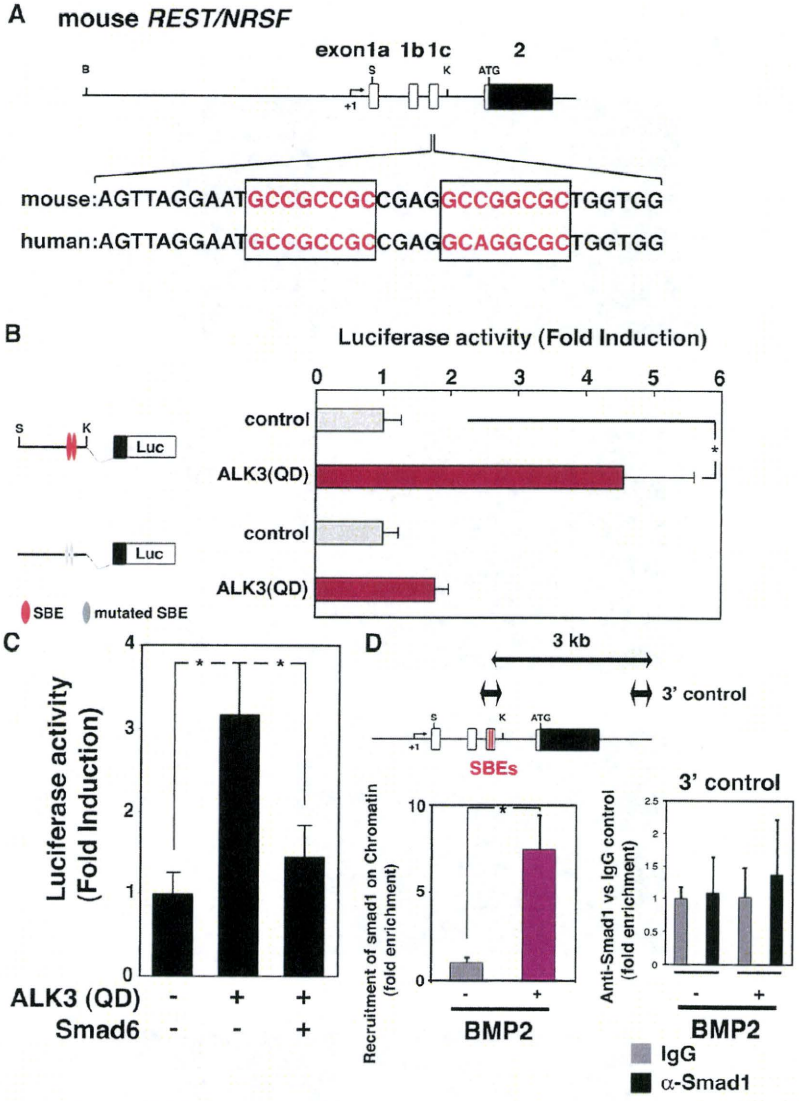

Figure 2. **Smad-dependent transactivation of the *REST/NRSF* gene.** (A) Comparison of a part of *REST/NRSF* genomic sequences between mouse and human. Part of the mouse *REST/NRSF* locus is shown on the top line, and sequence data around the SBEs in mouse and human are shown below. Boxed regions are sequences that match the SBE consensus. B, BamHI; S, SacI; K, KpnI. (B) Schematic representation of the *REST/NRSF* reporter constructs is shown on the left. NPCs were cotransfected with the reporter construct and pRL-CMV together with a control vehicle or a construct expressing ALK3(QD). Luciferase activity was measured 24 h after transfection. Mean ± SD (n = 3). Statistical significance was examined by Student's t test (*, $P < 0.05$). (C) NPCs were cotransfected with the *REST/NRSF* reporter construct and pRL-CMV along with the constructs indicated below the graph. Luciferase activity was measured 24 h after transfection. Mean ± SD (n = 3). Statistical significance was examined by Student's t test (*, $P < 0.05$). (D) NPCs were incubated with BMP2 (50 ng/ml) for 20 min and subjected to quantitative ChIP analysis using control IgG and anti-Smad1 antibodies (bottom left graph). Mean ± SD (n = 3). Statistical significance was examined by Student's t test (*, $P < 0.05$). Co-immunoprecipitated *REST/NRSF* gene fragments were amplified by PCR with a specific pair of primers. The amplified region is schematically indicated as the two-headed arrow spanning *REST/NRSF* exon 1c (top left). A primer set for amplification of a sequence 3 kb downstream of the SBEs in the *REST/NRSF* regulatory region (top right, two-headed arrow) was used to validate specific recruitment of Smad1 onto the SBEs (bottom right).

modification, i.e., acetylated histone H3 (AcH3) and trimethylation of histone H3-lysine 4 (H3K4me3; Jenuwein and Allis, 2001; Fig. S2 C). Collectively, it is conceivable that once *REST/NRSF* is activated by Smads, it no longer requires Smads for sustained expression during/after astrocytic differentiation.

REST/NRSF regulates fate specification of NPCs

In light of the above finding that REST/NRSF expression is induced by BMP2 stimulation, we anticipated that REST/NRSF would play a critical role in suppression of neuronal differentiation by BMP2. To test this, we infected NPCs with recombinant retroviruses engineered to express GFP (control) or GFP with REST/NRSF. Because we wanted to examine first whether REST/NRSF alone inhibits neuronal differentiation of NPCs, we switched the medium on the following day to one containing 0.5% FBS without bFGF to induce spontaneous differentiation, and cultured the cells for an additional 4 d. As shown in Fig. 3 A (top left), the cells infected with control viruses effectively differentiated into Map2ab-positive neurons (4 d: 31.8 ± 4.4%; 8 d: 42.1 ± 3.3%, right graph). In contrast, REST/NRSF expression in NPCs dramatically inhibited the cells from differentiating into neurons (Fig. 3 A, bottom left; 4 d: 5.8 ± 1.6%; 8 d: 13.5 ± 1.5%, right graph). Thus, although one might anticipate that REST/NRSF would not inhibit neuronal differentiation of NPCs but simply delays it, this is not the case: inhibition of neuronal differentiation by REST/NRSF was observed in both short and prolonged culture. Doublecortin (Dcx) and NeuN are known as early and late stage markers for neuronal differentiation, respectively. We found that REST/NRSF suppressed expression of both these neuronal markers (Fig. 3 B) suggesting, therefore, that REST/NRSF inhibits pan-neuronal differentiation of NPCs. As for astroglial differentiation, there was a slight increase of GFAP-positive astrocytes in the REST/NRSF-expressing virus-infected cells (Fig. 3 A; control, 4 d: 21.5 ± 4.0%; 8 d: 27.2 ± 3.3%; REST/NRSF, 4 d: 37.4 ± 2.5%; 8 d: 44.3 ± 0.84%, right graph).

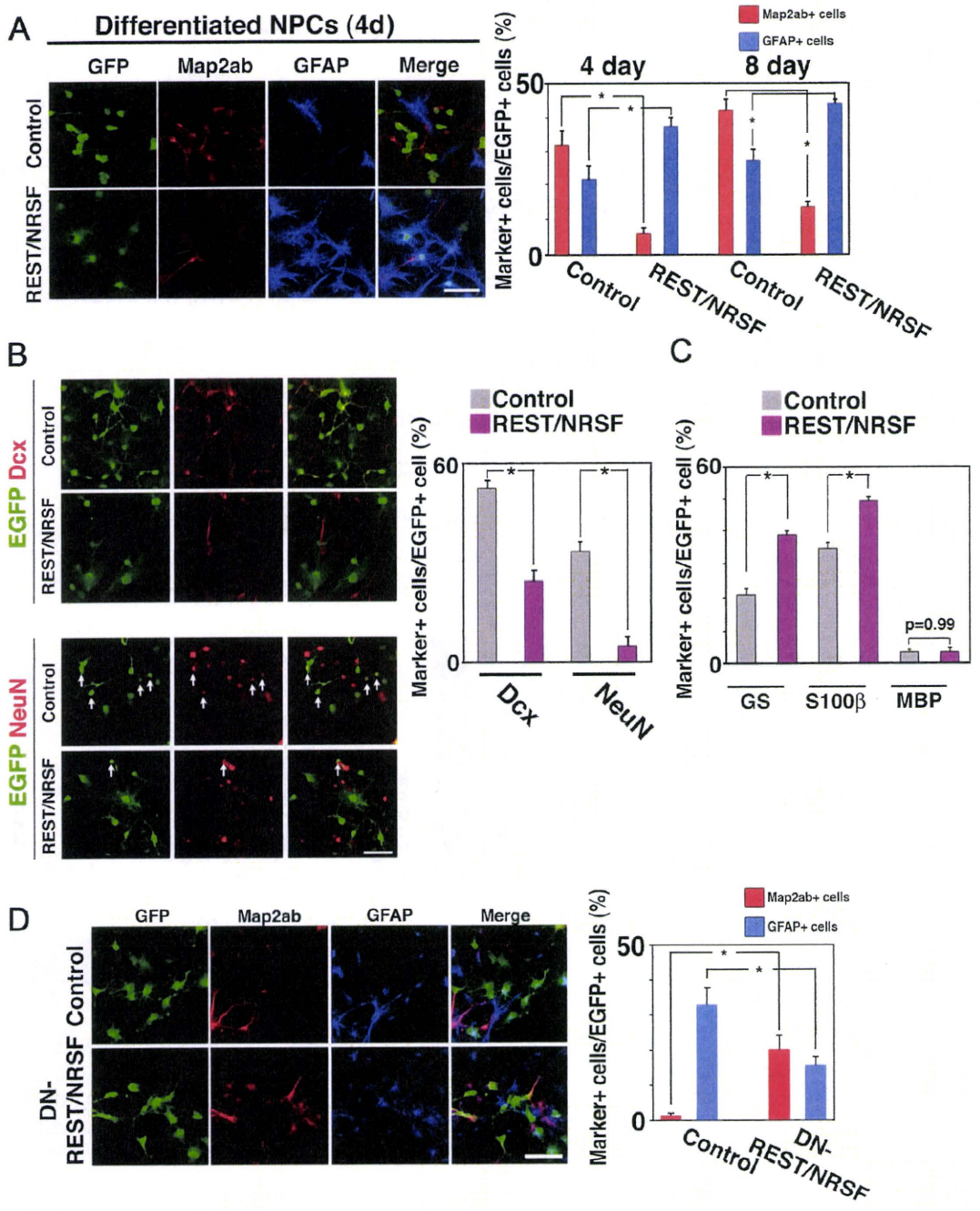

Figure 3. **REST/NRSF is sufficient to repress neuronal differentiation and is required for BMP2-induced suppression of neuronal differentiation of NPCs.** (A) NPCs were infected with recombinant retroviruses engineered to express only GFP (pMYs), or REST/NRSF together with GFP (REST/NRSF-pMYs), and cultured in medium supplemented with 0.5% FBS for 4 or 8 d to induce spontaneous differentiation. The cells were then stained with antibodies against GFP (green), Map2ab (red), and GFAP (blue). Bar, 50 μm. The percentage of marker-positive cells in each GFP-positive cell population after the 4-d culture was determined. Mean ± SD (n = 3). Statistical significance was examined by Student's t test (*, $P < 0.05$). (B) Expression of the neuronal markers NeuN and Dcx was examined in cells infected with control or REST/NRSF-expressing virus. The cells were subjected to immunocytochemical analysis after culturing in 0.5% FBS for 8 d (left). Bar, 20 μm. Marker-positive cells in total EGFP-positive cells were quantified (right). Mean ± SD (n = 3). Statistical significance was examined by Student's t test (*, $P < 0.05$). (C) Expression of the glial markers glutamine synthase (astrocytes), S100β (astrocytes), and MBP (oligodendrocytes) was examined in cells infected with control or REST/NRSF-expressing virus. The cells were subjected to immunocytochemical analysis after culturing with 0.5% FBS for 4 d. (D) NPCs were infected with viruses carrying control pMYs (GFP only), or DN-REST/NRSF-pMYs (DN-REST/NRSF) together with GFP, in culture medium containing bFGF (10 ng/ml), and subsequently treated with BMP2 (50 ng/ml) for 4 d. The cells were then stained with antibodies against GFP (green), Map2ab (red), and GFAP (blue). Bar, 50 μm. The percentage of marker-positive cells in each GFP-positive cell population after the 4-d culture was determined. Mean ± SD (n = 3). Statistical significance was examined by Student's t test (*, $P < 0.05$).

The effect of REST/NRSF on astrocytic differentiation of NPCs was further confirmed using two other astrocytic markers, glutamine synthetase (GS) (Tokunaga et al., 2004) and S100β (Fig. 3 C). There seemed to be a tendency for the number of astrocytic-marker–positive cells in NPCs infected with REST/NRSF-expressing virus to increase. However, there was no significant difference in the number of GFAP-positive cells between control and REST/NRSF-expressing virus-infected cells maintained in culture medium containing bFGF (Fig. S3 A), implying that the astrocyte-inducing activity of REST/NRSF is not strong enough to overcome the inhibitory effect of bFGF in NPC differentiation. Furthermore, the proliferation and cell death rates of control and REST/NRSF-expressing virus-infected cells were similar, as judged by BrdU uptake and cleaved caspase-3 staining (Fig. S3, B and C). To minimize the potent effect of BMPs contained in the serum, we used Noggin to inhibit functional BMP signaling in this experiment, and observed significant reduction of neuronal differentiation by REST/NRSF expression (Fig. S3 D). These observations suggest that REST/NRSF is able to function as a suppressor of neuronal differentiation in NPCs.

We next examined the requirement for REST/NRSF in the BMP-induced restriction of neuronal fate by means of a dominant-negative form of REST/NRSF harboring only its DNA-binding domain (DN-REST/NRSF; Chen et al., 1998). To this end, we infected NPCs with control and DN-REST/NRSF–expressing retroviruses, and cultured them with BMP2 for 4 d. As shown in Fig. 3 D, DN-REST/NRSF expression resulted in the derepression of neuronal fate, as judged by Map2ab expression. The control retrovirus-infected cells became Map2ab-positive neurons at a frequency of 1.3 ± 0.68%, whereas 20.2 ± 4.0% of DN-REST/NRSF–infected cells were Map2ab positive (Fig. 3 D). We did not observe significant influence on cell death rates by inhibition of REST/NRSF function (Fig. S3 E). These data imply that REST/NRSF expression is necessary and sufficient for the suppression of neuronal cell fate by BMP2.

Modulating REST/NRSF function perturbs astrocytic integrity

To test the idea that REST/NRSF might be a suppressor of inappropriate neuronal gene expression in astrocytes, we then examined the expression of REST/NRSF in primary cultured astrocytes derived from P0 mouse brain. We confirmed maturation of the astrocytes by determining the expression of glutamine transporter GLT-1 (Rothstein et al., 1994; Fig. S4 A). As shown in Fig. 4 A, REST/NRSF was expressed in GFAP-positive cultured astrocytes. We further examined REST/NRSF expression in vivo, and found that GS- and GFAP-positive astrocytes in postnatal day (P) 8 cortex expressed REST/NRSF (Fig. 4 B, Fig. S4 B). We further confirmed astrocytic expression of REST/NRSF compared with that in neurons by immunoblot analysis (Fig. S4 C).

To determine the function of REST/NRSF in astrocytes, we performed a luciferase assay using reporter constructs containing the *SCG10* minimal promoter with an intact or a mutated RE1/NRSE motif (Mori et al., 1990). If REST/NRSF had repressor activity in astrocytes, the luciferase activity in cells transfected with a DN-REST/NRSF–expressing construct should be higher than that in control vehicle-transfected cells. As shown in Fig. 4 C (left), astrocytes showed increased luciferase activity after introduction of the DN-REST/NRSF–expressing construct. Furthermore, derepression of the promoter was also observed by mutating the RE1/NRSE motif (Fig. 4 C, middle), indicating that endogenous REST/NRSF functions as a transcriptional repressor in astrocytes. In support of these findings, derepression of endogenous *SCG10* was detected when astrocytes were transfected with the DN-REST/NRSF–expressing construct (Fig. 4 C, right). To further confirm this repressor activity of REST/NRSF, we introduced the RE1/NRSE reporter into astrocytes and embryonic stem (ES) cells, which have been shown to express REST/NRSF (Ballas et al., 2005; Westbrook et al., 2008), and measured the reporter activity. As shown in Fig. 4 D, we found that the repressive activity of REST/NRSF was comparably strong in both ES cells and astrocytes, implying that REST/NRSF can function as a transcriptional repressor in other nonneural tissues or cell types. We also found recruitment of Smad1 to SBE-containing *REST/NRSF* regulatory region in ES cells (Fig. S4 D); therefore, the BMP-REST/NRSF axis apparently exists in other nonneural tissues.

The presence of repressive REST/NRSF activity in astrocytes prompted us to analyze the previously reported enrichment (Ballas et al., 2005) of endogenous REST/NRSF at its target loci. ChIP analysis revealed that REST/NRSF associated with several genes harboring RE1/NRSEs in astrocytes; in contrast, REST/NRSF binding to these target genes was negligible in neurons (Fig. 4 E).

In light of the above results, we then examined derepression of endogenous REST/NRSF target genes in astrocytes by perturbing REST/NRSF function. As shown in Fig. 5 A, transcriptional derepression of several endogenous REST/NRSF target genes was indeed observed in astrocytes transfected with the DN-REST/NRSF construct.

To determine the role played by REST/NRSF in restricting neuronal characteristics to maintain the cellular identity of astrocytes, we introduced DN-REST/NRSF into astrocytes and examined whether inappropriate expression of βIII-tubulin, a typical marker of neurons, occurred. As shown in Fig. 5 B, βIII-tubulin expression appeared in astrocytes with diminished REST/NRSF activity; we obtained a similar result using shRNA against REST/NRSF in astrocytes (Fig. S5, A–C). Another neuronal marker, Map2ab, was also expressed in DN-REST/NRSF–expressing astrocytes (Fig. 5 C).

Next, we investigated the in vivo significance of this inhibition of REST/NRSF function in astrocytes by injecting recombinant lentiviruses into the striatum of the adult mouse brain, and then examining βIII-tubulin expression in both EGFP- and S100β-positive virus-infected astrocytes 3 wk later. However, in the case of DN-REST/NRSF–expressing virus injection, we could not find any S100β-positive astrocytes that also expressed βIII-tubulin (0/107), suggesting that simple inhibition of REST/NRSF is not sufficient to induce ectopic neuronal marker expression in astrocytes in vivo. One might conclude that, although astrocytes in perinatal brain have been reported to retain broad differentiation potency (Laywell et al., 2000), astrocytes in the adult have lost the potential to express neuronal markers in response to a reduction of REST/NRSF expression.

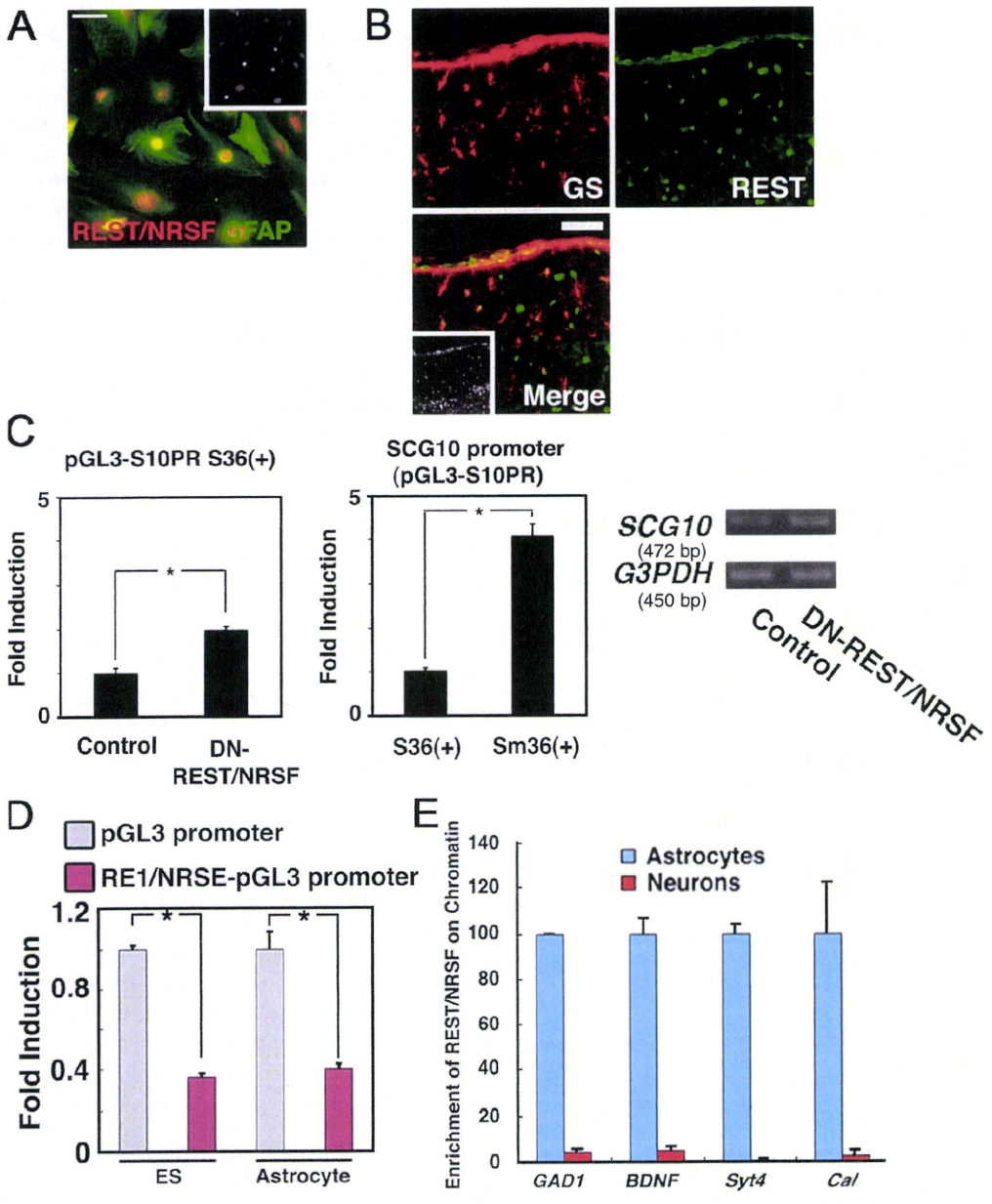

Figure 4. **Astrocytes express functional REST/NRSF.** (A) Expression of REST/NRSF in GFAP-positive astrocytes derived from P0 mouse brain. Bar, 50 μm. Inset: Hoechst nuclear staining of this field. (B) Expression of REST/NRSF in astrocytes in vivo. REST/NRSF (green) was expressed in GS (red)-positive cells in the cortical surface region of P8 mouse brain. Bar, 50 μm. Inset: Hoechst nuclear staining of the field. (C) REST/NRSF activity was examined using a reporter construct carrying the SCG10 minimal promoter (pGL3-S10PR) with intact (S36+) and mutated (Sm36+) RE1/NRSE. S36+ reporter activity was derepressed by the expression of DN-REST/NRSF in astrocytes (left). The reporter activity was enhanced by mutating the RE1/NRSE motif (middle). Mean ± SD ($n = 3$). Statistical significance was examined by Student's *t* test (*, $P < 0.05$). Endogenous expression of SCG10 was also examined by RT-PCR analysis in astrocytes introduced with control or DN-REST/NRSF-expressing vector (right). (D) Transcriptional suppressor activity of REST/NRSF was observed in astrocytes and ES cells as assessed by the RE1/NRSE reporter system. Mean ± SD ($n = 3$). Statistical significance was examined by Student's *t* test (*, $P < 0.05$). (E) Comparison, between neurons and astrocytes, of REST/NRSF association with RE1/NRSE-containing regions in *GAD1*, *BDNF*, *Synaptotagmin4* (*Syt4*), and *Calbindin* (*Cal*) genes, measured by quantitative ChIP analysis. Blue columns: astrocytes. Red columns: neurons. Mean ± SD.

Our results, however, show that this is not the case because expression of an ectopic neuronal marker was observed even in adult astrocytes when DN-REST/NRSF was expressed (Fig. S5, D and E). Therefore, the effects observed after introducing DN-REST/NRSF into astrocytes in vivo suggest either that 3 wk was not long enough or that other stimuli were required to reprogram astrocytes to express neuronal markers in vivo. In contrast to DN-REST/NRSF, REST/NRSF-VP16 (the DNA-binding domain fused to VP16) was efficient enough to increase the frequency of astrocytes positive for the neuronal marker in vivo (Fig. 5 D). Collectively, these results suggest that REST/NRSF acts as a substantial guardian of the astrocytic phenotype.

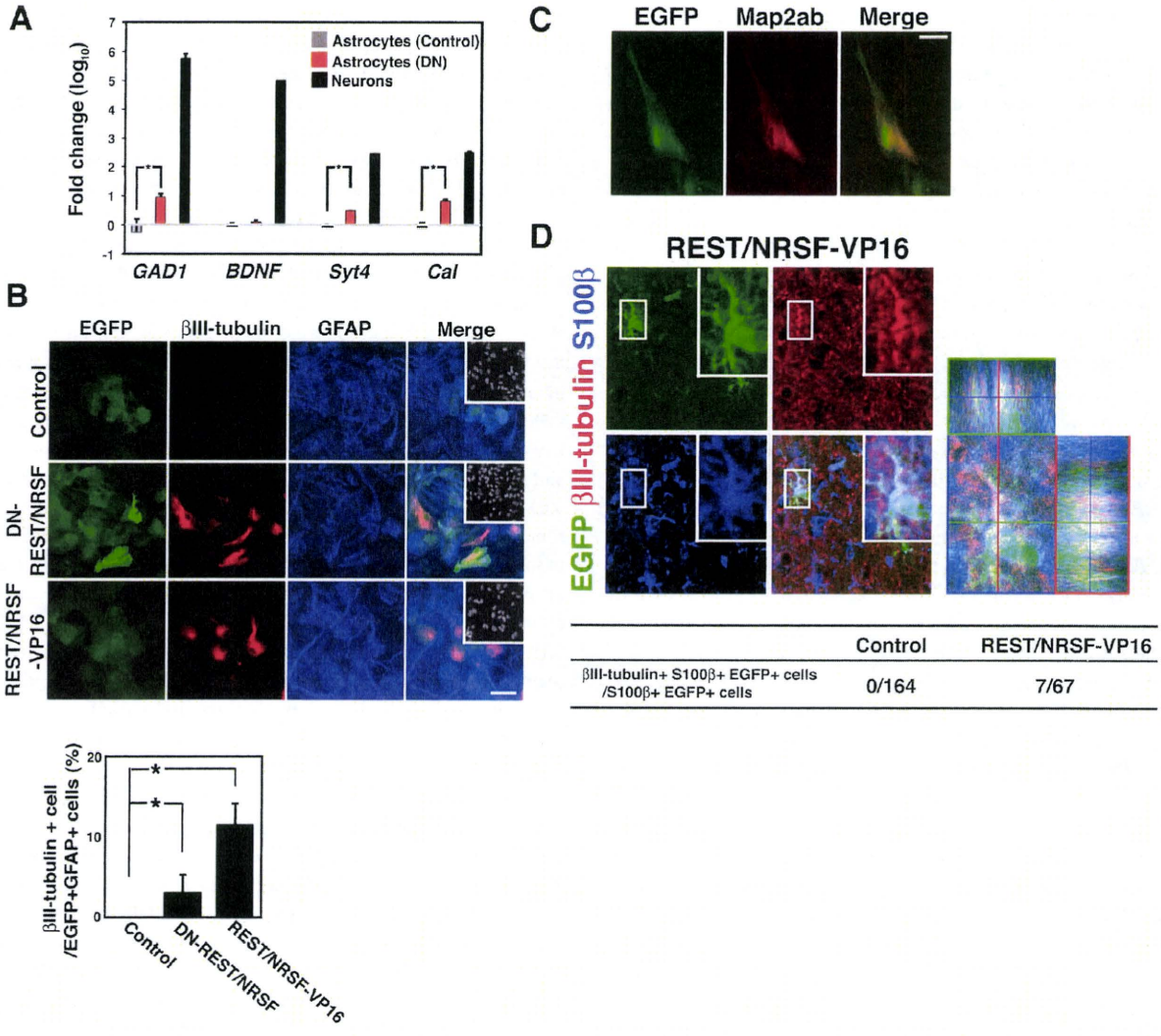

Figure 5. **Astrocytes are reprogrammed to express neuronal genes via perturbation of REST/NRSF function.** (A) Total RNAs were extracted from astrocytes transduced with control or DN-REST/NRSF–expressing vector, and from primary cultured neurons. These RNAs were then subjected to quantitative RT-PCR with primers specific for individual REST/NRSF target genes, *GAD1*, *BDNF*, *Syt4*, *and Cal*. (B) Expression of a neuronal marker in astrocytes after perturbation of REST/NRSF activity. Introduction of a DN-REST/NRSF–expressing construct into astrocytes resulted in ectopic expression of βIII-tubulin (red) in GFAP-positive (blue) astrocytes. Insets: Hoechst nuclear staining of each field. Bar, 50 μm. The percentage of βIII-tubulin–positive cells in GFP- and GFAP-positive populations was determined (right graph); the effect of REST/NRSF-VP16 in astrocytes is also indicated. Mean ± SD (n = 3). Statistical significance was examined by Student's t test (*, $P < 0.05$). (C) Expression of Map2ab in DN-REST/NRSF-expressing astrocytes. Astrocytes were cultured as in B and stained with anti-GFP and -Map2ab antibodies. (D) Ectopic expression of neuronal markers in S100β-positive astrocytes in vivo after introduction of REST/NRSF-VP16. Lentiviruses were injected stereotactically into the striatum of adult mouse brain, followed by immunohistochemical analysis 3 wk after the surgery. Insets: higher magnification image of boxed region in each field. Quantification is shown in the table (Control, 164 S100β+/EGFP+ cells from three animals; REST/NRSF-VP16, 67 S100β+/EGFP+ cells from three animals).

Discussion

Our objective in the present study was to determine how, during a cell's progression toward a particular restricted lineage (here, astrocytes), characters that are specific to an alternative lineage (neurons) are suppressed. Contribution of BMP signaling to NPC differentiation has also been examined by several genetic manipulations of BMP receptors. Although the conditional knockout of BMP type IA receptor (BMPRIA) in cortex showed minor effects on glial differentiation (Araya et al., 2008), compound disruption of BMPRIA and BMPRIB in mice resulted in a decreased number of astrocytes generated from NPCs (See et al., 2007). Moreover, several lines of evidence suggested that BMP2 is a strong astrocyte-inducing cytokine for NPCs in vitro (Nakashima et al., 1999b, 2001; Mehler et al., 2000; See et al., 2007). BMPs have also been shown to not only induce GFAP expression, but also to advance maturation of astrocytes, i.e., BMPs induce cell cycle exit and loss of NPC markers (Bonaguidi et al., 2005). Therefore, we thought that unraveling the molecular mechanisms of astrocyte differentiation and maturation induced by the activation of BMP signaling may elucidate the machinery that restricts differentiation plasticity in astrocytes.

As we reported previously, BMP2 triggers the expression of negative HLH genes (Ids and Hes5), resulting in the inhibition of such neurogenic bHLHs as Mash1 and Neurogenin. However, BMP2-induced up-regulation of these negative HLH factors in NPCs is transient (Nakashima et al., 2001; Fig. S1, D and E), and their expression is normally detected in the germinal zone of the developing brain, where undifferentiated cells are located (Duncan et al., 1992; Ellmeier and Weith, 1995; Lyden et al., 1999). Thus, we wished to identify a bona fide suppressor of neuronal phenotype that acts both during and after astrocyte differentiation. Although REST/NRSF is known as a major regulator of neuronal genes in nonneuronal tissues, and its expression is regulated during development (Chong et al., 1995), the precise regulation of *REST/NRSF* expression by itself has not been addressed in detail. In this study, we have now identified REST/NRSF as a BMP-regulated factor that suppresses neuronal differentiation. The transcriptional up-regulation of *REST/NRSF* by BMP signaling is mediated by the direct binding of Smad transcription factors to the SBEs in the *REST/NRSF* regulatory region (Fig. 2). Although a direct link between BMP signaling and *REST/NRSF* expression was not shown, it was recently reported that REST/NRSF expression is observed in the ectoderm of early *Xenopus* embryos where BMP signaling is known to modulate tissue patterning, and that the interference of REST/NRSF mimics several features associated with a decreased BMP function (Olguín et al., 2006). Thus, the BMP-REST/NRSF axis may exist in broader aspects of tissue organogenesis. Although we used BMP2 in the present study to examine the inhibition of neuronal differentiation of NPCs, other BMP family members, such as BMP4 and BMP7, also signal through the type IA receptor and generally exert similar effects to those of BMP2 (Yanagisawa et al., 2001). Considering this functional conservation, other type IA–using BMPs may also be able to induce *REST/NRSF* expression.

Unlike that of Ids and Hes5, expression of REST/NRSF is maintained even in differentiated astrocytes (Fig. 1 C and Fig. 4 B), yet how this difference occurs is currently unknown. REST/NRSF is known to be regulated by canonical Wnt signaling (Nishihara et al., 2003), and certain types of astrocytes secrete Wnt3 to provide a niche for adult NPCs (Lie et al., 2005). It will therefore be of interest to test whether activation of Wnt pathways plays crucial roles, whether autocrine or paracrine, to maintain an astrocytic niche. An alternative possibility is that REST/NRSF expression is maintained by mammalian SWI/SNF chromatin remodeling complexes (Martens and Winston, 2003) after a transcriptional priming effect supplied by the BMP–Smad pathway. Brg1, one of the two catalytic ATPase subunits of the SWI/SNF complex, has been shown using CNS-specific *Brg1* knockout animals to be required for gliogenesis (Matsumoto et al., 2006). Nevertheless, the contribution of SWI/SNF complex to REST/NRSF expression and repression of neuronal genes in differentiated astrocytes must await future study in an animal model of glia-specific depletion of *Brg1*.

Similar to Ids, as reported in our previous study (Nakashima et al., 2001), the expression of REST/NRSF in NPCs does not seem to actively induce astrogliogenesis because forced expression of REST/NRSF alone was unable to induce GFAP-positive astrocytic differentiation (Fig. S3 A). The contribution of REST/NRSF to an early step of astrocytic differentiation may be exerted by repression either of neurogenic bHLH factors such as *NeuroD* (Lunyak et al., 2002; Otto et al., 2007), or of an orphan nuclear receptor like *Tlx* (Otto et al., 2007); the transcriptional repressor Tlx represses astrocyte differentiation (Miyawaki et al., 2004; Shi et al., 2004; Uemura et al., 2006), in part by binding directly to the promoter region of the astrocytic gene *gfap* (Shi et al., 2004). Because we did not observe active promotion of astroglial differentiation of NPCs by REST/NRSF overexpression (Fig. S3 A), we cannot rule out the possibility that REST/NRSF-induced suppression of genes which repress astrocyte differentiation is involved in BMP2-induced astrogliogenesis. Considering that RE1/NRSE motifs have been identified in hundreds of neuronal genes, including ion channels, neurotransmitter receptors, neurotrophins, synaptic vesicle proteins, and cytoskeletal and adhesion molecules (Bruce et al., 2004), REST/NRSF potentially could suppress a diverse array of neuronal genes simultaneously. Therefore, although REST/NRSF induction is probably sufficient for the inhibition of neuronal differentiation, it is conceivable that BMP signaling needs to collaborate with other signaling pathways such as the JAK/STAT pathway (Nakashima et al., 1999a; He et al., 2005) for effective induction of astrocyte differentiation.

Once cells acquire the properties of a particular lineage, they specifically repress genes that are expressed in alternative cell lineages. This restriction of cellular plasticity must be tightly regulated to ensure cellular or tissue homeostasis. In the case of neurons, astrocytic gene expression is, in part, repressed by epigenetic modification through DNA methylation (Takizawa et al., 2001; Setoguchi et al., 2006; Kohyama et al., 2008; Namihira et al., 2009). As shown in Figs. 1, 4, and S1 E, expression of REST/NRSF is up-regulated and maintained during astrocyte differentiation, and REST/NRSF is bound to various kinds of neuronal genes in differentiated astrocytes (Fig. 4 E). We have here provided evidence that perturbing the function of REST/NRSF by both DN-REST/NRSF and REST/NRSF-VP16 resulted in ectopic neuronal marker expression in astrocytes in vitro (Fig. 5 A). However, we could not observe βIII-tubulin expression in astrocytes in vivo by simple inhibition of REST/NRSF function with DN-REST/NRSF, whereas REST/NRSF-VP16 was able to induce the neuronal marker ectopically. This difference between the two REST/NRSF mutants may be caused by as-yet-unknown mechanisms that are functioning to further repress neuronal genes in astrocytes in vivo. Although we must await further investigation to identify these mechanisms, it is conceivable that REST/NRSF plays at least some part in restricting the differentiation plasticity of astrocytes by suppressing neuronal gene expression. However, we have not yet been able to rule out the possibility that off-target variable effects of REST/NRSF-VP16 contribute to ectopic neuronal gene expression in astrocytes in vivo.

Materials and methods

Cell culture

NPCs were prepared from embryonic day (E) 14 mouse telencephalons as described previously (Nakashima et al., 1999b). Freshly isolated cells were plated onto dishes precoated with poly-L-ornithine (Sigma-Aldrich)

and fibronectin (Sigma-Aldrich) and cultured in N2-supplemented DME/F-12 medium (N2/DME/F12) with 10 ng/ml basic fibroblast growth factor (bFGF; PeproTech) for 4 d. bFGF was included unless otherwise indicated. Cells were then detached and replated onto 8-well chamber slides (Thermo Fisher Scientific) precoated with poly-L-ornithine and fibronectin (6×10^4 cells per well) and 12-well plates (4×10^5 cells per well; Thermo Fisher Scientific) for immunocytochemistry and luciferase assay, respectively. Primary astrocytes from cortex of postnatal day (P) 0 and adult mice were prepared essentially as described previously (Song et al., 2002). In brief, confluent astrocytes in medium were treated with 20 μM cytosine arabinoside for 72 h to eliminate proliferating cells, followed by recovery in fresh medium for 24 h. Under these conditions, most of the cells were GFAP-positive astrocytes with little contamination by other cell types. Maturation of astrocytes was assessed by examining the expression of glutamine transporter GLT-1 (Rothstein et al., 1994). Primary neurons from E14 cortex were prepared as described previously (Martinowich et al., 2003).

Immunocytochemistry

Cells cultured on coated chamber slides were washed with PBS, fixed in 4% paraformaldehyde (PFA) in PBS, and stained with one of the following primary antibodies: rabbit anti-GFAP (1:1,500; Dako), rabbit anti-REST/NRSF (1:500; Millipore), rabbit anti-GFP (1:1,000; MBL), rat anti-GFP (1:200; Nacalai Tesque), mouse anti–microtubule-associated proteins 2a and 2b (MAP2ab) (1:1,000; Sigma-Aldrich), mouse anti-Nestin (1:1,000; Millipore), mouse anti-S100β (1:1,000; Sigma-Aldrich), guinea pig anti-GFAP (1:2,000; Advanced Immunochemical), guinea pig anti-GLT1 (Millipore), mouse anti-GS (BD), rabbit anti-Id1 (1:100; Santa Cruz Biotechnology, Inc.), and rabbit anti-cleaved caspase-3 (Asp175; 1:500; Cell Signaling Technology). The following secondary antibodies were used: Alexa 488–conjugated goat anti–mouse IgG (1:500; Invitrogen), Cy3-conjugated goat anti–mouse IgG (1:500; Jackson ImmunoResearch Laboratories, Inc.), Alexa 488–conjugated goat anti–rabbit (1:500; Invitrogen), FITC-conjugated donkey anti–rat (1:500; Jackson ImmunoResearch Laboratories, Inc.), FITC-conjugated donkey anti–guinea pig (1:500; Jackson ImmunoResearch Laboratories, Inc.), Cy3-conjugated donkey anti–rabbit (1:250; Jackson ImmunoResearch Laboratories, Inc.), and Cy5-conjugated donkey anti–guinea pig (1:250; Jackson ImmunoResearch Laboratories, Inc.). Nuclei were stained using bisbenzimide H33258 fluorochrome trihydrochloride (Nacalai Tesque). The fluorescence images were acquired using a fluorescence microscope (Axiovert 200M; Carl Zeiss, Inc.), 20x and 40x objectives, and LSM Image Browser software. Images were combined for figures using Adobe Photoshop CS. All experiments were independently replicated at least three times.

Immunohistochemistry

P8 pups were perfused through the left ventricle with 4% PFA in PBS (pH 7.4). Brains were dissected out and postfixed overnight at 4°C, cryoprotected in 30% sucrose in PBS overnight at 4°C, and then embedded in OCT compound (Tissue Tek). Cryostat sections (12 μm) were cut and affixed to APS-coated glass slides (Matsunami Glass). The sections were then permeabilized in TBS-T (TBS containing 0.05% Tween 20) for 10 min and blocked with 10% normal donkey serum (Millipore) in PBS for 1 h at room temperature. The sections were reacted overnight at 4°C with primary antibodies in blocking solution. After three washes with PBS, the sections were incubated in PBS containing the secondary antibodies for 1 h. Optical sections were viewed using a scanning-laser confocal imaging system (LSM510; Carl Zeiss, Inc.) with 40x and 63x objectives. Image acquisition was performed with LSM Image Browser software (Carl Zeiss, Inc.). Images were combined for figures using Adobe Photoshop CS.

RNA isolation and reverse-transcription PCR (RT-PCR)

Total RNAs were isolated using Sepasol RNAI (Nacalai Tesque) and treated with DNase I (Promega). First-strand cDNAs were synthesized from 1 μg total RNA with Superscript II (Invitrogen). The RT products (1 μl) were used as templates for PCR amplification (AmpliTaq Gold; Applied Biosystems) in 25 μl reaction solution containing 2 μM gene-specific primers. Quantitative real-time PCR was performed in MX3000p (Agilent Technologies) using SYBR-Green PCR Master Mix (Takara Bio Inc.). The gene-specific primers were as follows: mouse REST/NRSF: REST-S, 5′-gaactcacacaggagaacgcc-3′; REST-AS, 5′-gattacacttcttagaagccg-3′; mouse G3PDH: G3PDH-S, 5′-accacagtccatgccatcac-3′; G3PDH-AS, 5′-tccaccaccctgttgctgta-3′; mouse SCG10: SCG10-S, 5′-gagctgtctatgctgtcactg-3′; SCG10-AS, 5′-tgttcctgcgaacctctgca-3′; mouse Hes5: Hes5-S, 5′-aagagcctgcaccaggacta-3′; Hes5-AS, 5′-cgctggaagtggtaaagca-3′; mouse Id1: Id1-S, 5′-ggtggatccaccatgaaggtcgccagtg-3′; Id1-AS, 5′-ggtggatccgtccatctggtccctcagtgc-3′. For analysis of the REST/NRSF target genes *GAD1*, *BDNF*, *Synaptotagmin4*, and *Calbindin*, primer sets were designed according to a previous report (Ballas et al., 2005).

Western blot analysis

Western blot analysis was performed by an established method. 20-μg protein samples of each total cell extract were separated by 5–20% gradient SDS-PAGE, transferred to a nitrocellulose membrane, and probed with anti-REST (rabbit IgG, Millipore), anti–β-actin (mouse IgG; Sigma-Aldrich), anti-Smad1 (mouse IgG; Santa Cruz Biotechnology, Inc.), and anti-phosphorylated Smad1/5/8 (Cell Signaling Technology) antibodies. Signals were detected with HRP-conjugated secondary antibodies (Jackson ImmunoResearch Laboratories, Inc.) using an ECL kit (GE Healthcare). The amounts of proteins loaded in each slot were normalized to those of β-actin.

Luciferase assay

NPCs, primary astrocytes, and ES cells were transfected with luciferase reporter plasmids, pGL3 promoter (Promega) with or without RE1/NRSE (5′-TTCAGCACCACGGACAGCGCC-3′), using Trans-IT LT-1 (Mirus) or Lipofectamine 2000 (Invitrogen) according to the manufacturer's protocol. Luciferase reporter constructs with a REST/NRSF gene regulatory fragment (+65 bp to +1607 bp) or harboring Smad binding element mutations were used. To manipulate BMP signaling, three expression constructs were also used: smad6 (inhibitory smad) and ALK3QD (constitutively activated BMP type I receptor) cDNA inserted into pMY vector (Morita et al., 2000), DN-Smad1 in pCI vector (Promega). As an internal control, a plasmid containing a sea pansy luciferase expression construct (pRL-CMV; Promega) was cotransfected with the reporter constructs described above. To evaluate repressor activity of REST/NRSF on *SCG10*, pGL3-basic vectors carrying a minimum promoter region of *SCG10* with intact (pGL3-S10PR S36(+); 5′-TTCAGCACCACGGAGAGTGCC-3′) and mutated (pGL3-S10PR Sm36(+); 5′-TTCAGCACCACTTAGAGTGCC-3′) RE1/NRSE were also used (underlined GG dinucleotides were substituted by TT dinucleotides). On the following day, cells were solubilized and luciferase activity was measured according to the procedures recommended for the dual luciferase reporter assay system (Promega). ARVO (PerkinElmer) was used for quantification.

Recombinant retrovirus construction and infection

cDNAs encoding full-length mouse REST/NRSF and its DNA-binding domain were cloned into expression vector pMY containing an internal ribosome entry site followed by the region upstream of the GFP gene (Kitamura et al., 2003). The Plat-E packaging cell line was transiently transfected with this construct by Trans-IT 293 (Mirus). On the following day, the medium was replaced with N2/DMEM/F12 and the cells were cultured in this medium for 1 d before virus was collected.

Lentivirus construction and infection

The DNA-binding domain of REST/NRSF and the DNA-binding domain of REST/NRSF fused with VP16 were subcloned into CSC PW lentiviral vector (Kuwabara et al., 2004). The production and infection of lentivirus followed previous reports (Miyoshi et al., 1999; Kohyama et al., 2005). The shRNA sequence targeted for *REST/NRSF* was 5′-gaggcagtctcttcaacaa-3′. This shRNA cassette was subcloned into CSC PW lentiviral vector containing both CMV-EGFP and murine U6 promoter cassettes derived from the original CSC PW plasmid (Kuwabara et al., 2004). Lentiviruses (200 nl) were stereotactically injected into the striatum of the adult mouse brain (0 mm anterior, ± 2 mm lateral to bregma, and 2.9 mm below the brain surface).

Chromatin immunoprecipitation assay

Chromatin immunoprecipitation (ChIP) was performed according to a protocol published by Upstate Biotechnology. Undifferentiated NPCs and differentiated cells were exposed to formaldehyde, at a final concentration of 1%, added directly to the tissue culture medium. Co-immunoprecipitated DNA was used as a template for PCR of the genomic region containing two smad-binding elements in the *REST/NRSF* gene with the following sets of primers: REST/NRSF chipS (5′-GCCCAAGTTTGCAAAGAGCTG-3′) and REST/NRSF chipAS (5′-CAACAAAAAGTTGAGCCCGAATG-3′). Quantitative real-time PCR was performed in the Mx3000p system (Agilent Technologies) using SYBR-Green PCR Master Mix (Takara Bio Inc.). For analysis of REST/NRSF target genes including *GAD1*, *BDNF*, *Synaptotagmin4*, and *Calbindin*, primer sets were designed according to a previous report (Ballas et al., 2005). Antibodies used for the ChIP assay were rabbit anti-REST/NRSF (Millipore), mouse anti-Smad1 (Santa Cruz Biotechnology, Inc.), rabbit anti-acetylated histone H3 (Millipore), rabbit anti-trimethylated histone H3-lysine 4 (Abcam), and mouse/rabbit control IgGs (Santa Cruz Biotechnology, Inc.).

Online supplemental material

Fig. S1 shows that phosphorylation of Smad1/5/8 induced by BMP2 exposure in NPCs and the effect of BMP2 on oligodendrocyte differentiation of NPCs. Expression kinetics of BMP signaling-target genes are also shown.

Fig. S2 shows reporter assays using a dominant-negative form of Smad1 and ChIP assays using antibodies against Smad1, H3K4me3, and AcH3 in NPCs, astrocytes, and neurons. Fig. S3 shows the effect of REST/NRSF or DN-REST/NRSF expression on cell proliferation and cell death in NPCs. Fig. S4 shows expression of GLT-1 in cultured astrocytes and REST/NRSF expression in the different regions of mouse brain. Smad1 occupancy in *REST/NRSF* regulatory region in ES cells is shown. Fig. S5 A shows a knockdown study using an RNAi approach in cultured astrocytes. We also show the effect of DN-REST/NRSF in cultured astrocytes derived from adult mice. Online supplemental material is available at http://www.jcb.org/cgi/content/full/jcb.200908048/DC1.

We thank Dr. T. Kitamura (Tokyo University) for pMX vector and Plat-E cells; Dr. A. Smith (Cambridge University) for ES cells; Dr. H. Mori (Nagasaki University) for REST TRSF promoter, SCG10 promoter and REST TRSF expression vector; Dr. R. Nageyama for DN-Smad1 construct; and Astellas Pharma for BMP2. We appreciate Drs. T. Sunabori, A. Hamihira, H. Bessho, and T. Matsui for valuable discussions. We also thank Dr. I. Smith for helpful comments and critical reading of the manuscript. We are very grateful to H. Ueda and M. Tano for excellent secretarial assistance. Many thanks to S. Urayama and H. Hamihira for technical help.

This work has been supported by a Grant-in-Aid for Young Scientists (Start-up) and a Grant-in-Aid for Scientific Research on Priority Areas-Molecular Brain Science, and the NAIST Global COE Program (Frontier Biosciences: Strategies for survival and adaptation in a changing global environment) from the Ministry of Education, Culture, Sports, Science and Technology of Japan.

Submitted: 10 August 2009
Accepted: 4 March 2010

References

Araya, R., M. Kudo, M. Kawano, K. Ishii, T. Hashikawa, T. Iwasato, S. Itohara, T. Terasaki, A. Oohira, Y. Mishina, and M. Yamada. 2008. BMP signaling through BMPRIA in astrocytes is essential for proper cerebral angiogenesis and formation of the blood-brain-barrier. *Mol. Cell. Neurosci.* 38:417–430. doi:10.1016/j.mcn.2008.04.003

Ballas, N., E. Battaglioli, F. Atouf, M.E. Andres, J. Chenoweth, M.E. Anderson, C. Burger, M. Moniwa, J.R. Davie, W.J. Bowers, et al. 2001. Regulation of neuronal traits by a novel transcriptional complex. *Neuron.* 31:353–365. doi:10.1016/S0896-6273(01)00371-3

Ballas, N., C. Grunseich, D.D. Lu, J.C. Speh, and G. Mandel. 2005. REST and its corepressors mediate plasticity of neuronal gene chromatin throughout neurogenesis. *Cell.* 121:645–657. doi:10.1016/j.cell.2005.03.013

Bertrand, N., D.S. Castro, and F. Guillemot. 2002. Proneural genes and the specification of neural cell types. *Nat. Rev. Neurosci.* 3:517–530. doi:10.1038/nrn874

Bonaguidi, M.A., T. McGuire, M. Hu, L. Kan, J. Samanta, and J.A. Kessler. 2005. LIF and BMP signaling generate separate and discrete types of GFAP-expressing cells. *Development.* 132:5503–5514. doi:10.1242/dev.02166

Bonni, A., Y. Sun, M. Nadal-Vicens, A. Bhatt, D.A. Frank, I. Rozovsky, N. Stahl, G.D. Yancopoulos, and M.E. Greenberg. 1997. Regulation of gliogenesis in the central nervous system by the JAK-STAT signaling pathway. *Science.* 278:477–483. doi:10.1126/science.278.5337.477

Bruce, A.W., I.J. Donaldson, I.C. Wood, S.A. Yerbury, M.I. Sadowski, M. Chapman, B. Göttgens, and N.J. Buckley. 2004. Genome-wide analysis of repressor element 1 silencing transcription factor/neuron-restrictive silencing factor (REST/NRSF) target genes. *Proc. Natl. Acad. Sci. USA.* 101:10458–10463. doi:10.1073/pnas.0401827101

Chen, Z.F., A.J. Paquette, and D.J. Anderson. 1998. NRSF/REST is required in vivo for repression of multiple neuronal target genes during embryogenesis. *Nat. Genet.* 20:136–142. doi:10.1038/2431

Chong, J.A., J. Tapia-Ramírez, S. Kim, J.J. Toledo-Aral, Y. Zheng, M.C. Boutros, Y.M. Altshuller, M.A. Frohman, S.D. Kraner, and G. Mandel. 1995. REST: a mammalian silencer protein that restricts sodium channel gene expression to neurons. *Cell.* 80:949–957. doi:10.1016/0092-8674(95)90298-8

Conaco, C., S. Otto, J.J. Han, and G. Mandel. 2006. Reciprocal actions of REST and a microRNA promote neuronal identity. *Proc. Natl. Acad. Sci. USA.* 103:2422–2427. doi:10.1073/pnas.0511041103

Duncan, M., E.M. DiCicco-Bloom, X. Xiang, R. Benezra, and K. Chada. 1992. The gene for the helix-loop-helix protein, Id, is specifically expressed in neural precursors. *Dev. Biol.* 154:1–10. doi:10.1016/0012-1606(92)90042-F

Ellmeier, W., and A. Weith. 1995. Expression of the helix-loop-helix gene Id3 during murine embryonic development. *Dev. Dyn.* 203:163–173.

Gage, F.H. 2000. Mammalian neural stem cells. *Science.* 287:1433–1438. doi:10.1126/science.287.5457.1433

Gradwohl, G., C. Fode, and F. Guillemot. 1996. Restricted expression of a novel murine atonal-related bHLH protein in undifferentiated neural precursors. *Dev. Biol.* 180:227–241. doi:10.1006/dbio.1996.0297

He, F., W. Ge, K. Martinowich, S. Becker-Catania, V. Coskun, W. Zhu, H. Wu, D. Castro, F. Guillemot, G. Fan, et al. 2005. A positive autoregulatory loop of Jak-STAT signaling controls the onset of astrogliogenesis. *Nat. Neurosci.* 8:616–625. doi:10.1038/nn1440

Hsieh, J., and F.H. Gage. 2004. Epigenetic control of neural stem cell fate. *Curr. Opin. Genet. Dev.* 14:461–469. doi:10.1016/j.gde.2004.07.006

Huang, Y., S.J. Myers, and R. Dingledine. 1999. Transcriptional repression by REST: recruitment of Sin3A and histone deacetylase to neuronal genes. *Nat. Neurosci.* 2:867–872. doi:10.1038/13165

Imamura, T., M. Takase, A. Nishihara, E. Oeda, J. Hanai, M. Kawabata, and K. Miyazono. 1997. Smad6 inhibits signalling by the TGF-beta superfamily. *Nature.* 389:622–626. doi:10.1038/39355

Jenuwein, T., and C.D. Allis. 2001. Translating the histone code. *Science.* 293:1074–1080. doi:10.1126/science.1063127

Johnson, R., R.J. Gamblin, L. Ooi, A.W. Bruce, I.J. Donaldson, D.R. Westhead, I.C. Wood, R.M. Jackson, and N.J. Buckley. 2006. Identification of the REST regulon reveals extensive transposable element-mediated binding site duplication. *Nucleic Acids Res.* 34:3862–3877. doi:10.1093/nar/gkl525

Kitamura, T., Y. Koshino, F. Shibata, T. Oki, H. Nakajima, T. Nosaka, and H. Kumagai. 2003. Retrovirus-mediated gene transfer and expression cloning: powerful tools in functional genomics. *Exp. Hematol.* 31:1007–1014.

Koenigsberger, C., J.J. Chicca II, M.C. Amoureux, G.M. Edelman, and F.S. Jones. 2000. Differential regulation by multiple promoters of the gene encoding the neuron-restrictive silencer factor. *Proc. Natl. Acad. Sci. USA.* 97:2291–2296. doi:10.1073/pnas.050578797

Kohyama, J., A. Tokunaga, Y. Fujita, H. Miyoshi, T. Nagai, A. Miyawaki, K. Nakao, Y. Matsuzaki, and H. Okano. 2005. Visualization of spatiotemporal activation of Notch signaling: live monitoring and significance in neural development. *Dev. Biol.* 286:311–325. doi:10.1016/j.ydbio.2005.08.003

Kohyama, J., T. Kojima, E. Takatsuka, T. Yamashita, J. Namiki, J. Hsieh, F.H. Gage, M. Namihira, H. Okano, K. Sawamoto, and K. Nakashima. 2008. Epigenetic regulation of neural cell differentiation plasticity in the adult mammalian brain. *Proc. Natl. Acad. Sci. USA.* 105:18012–18017. doi:10.1073/pnas.0808417105

Kojima, T., K. Murai, Y. Naruse, N. Takahashi, and N. Mori. 2001. Cell-type non-selective transcription of mouse and human genes encoding neural-restrictive silencer factor. *Brain Res. Mol. Brain Res.* 90:174–186. doi:10.1016/S0169-328X(01)00107-3

Kusanagi, K., H. Inoue, Y. Ishidou, H.K. Mishima, M. Kawabata, and K. Miyazono. 2000. Characterization of a bone morphogenetic protein-responsive Smad-binding element. *Mol. Biol. Cell.* 11:555–565.

Kuwabara, T., J. Hsieh, K. Nakashima, K. Taira, and F.H. Gage. 2004. A small modulatory dsRNA specifies the fate of adult neural stem cells. *Cell.* 116:779–793. doi:10.1016/S0092-8674(04)00248-X

Laywell, E.D., P. Rakic, V.G. Kukekov, E.C. Holland, and D.A. Steindler. 2000. Identification of a multipotent astrocytic stem cell in the immature and adult mouse brain. *Proc. Natl. Acad. Sci. USA.* 97:13883–13888. doi:10.1073/pnas.250471697

Lie, D.C., S.A. Colamarino, H.J. Song, L. Désiré, H. Mira, A. Consiglio, E.S. Lein, S. Jessberger, H. Lansford, A.R. Dearie, and F.H. Gage. 2005. Wnt signalling regulates adult hippocampal neurogenesis. *Nature.* 437:1370–1375. doi:10.1038/nature04108

Lunyak, V.V., R. Burgess, G.G. Prefontaine, C. Nelson, S.H. Sze, J. Chenoweth, P. Schwartz, P.A. Pevzner, C. Glass, G. Mandel, and M.G. Rosenfeld. 2002. Corepressor-dependent silencing of chromosomal regions encoding neuronal genes. *Science.* 298:1747–1752. doi:10.1126/science.1076469

Lyden, D., A.Z. Young, D. Zagzag, W. Yan, W. Gerald, R. O'Reilly, B.L. Bader, R.O. Hynes, Y. Zhuang, K. Manova, and R. Benezra. 1999. Id1 and Id3 are required for neurogenesis, angiogenesis and vascularization of tumour xenografts. *Nature.* 401:670–677. doi:10.1038/44334

Martens, J.A., and F. Winston. 2003. Recent advances in understanding chromatin remodeling by Swi/Snf complexes. *Curr. Opin. Genet. Dev.* 13:136–142. doi:10.1016/S0959-437X(03)00022-4

Martinowich, K., D. Hattori, H. Wu, S. Fouse, F. He, Y. Hu, G. Fan, and Y.E. Sun. 2003. DNA methylation-related chromatin remodeling in activity-dependent BDNF gene regulation. *Science.* 302:890–893. doi:10.1126/science.1090842

Matsumoto, S., F. Banine, J. Struve, R. Xing, C. Adams, Y. Liu, D. Metzger, P. Chambon, M.S. Rao, and L.S. Sherman. 2006. Brg1 is required for murine neural stem cell maintenance and gliogenesis. *Dev. Biol.* 289:372–383. doi:10.1016/j.ydbio.2005.10.044

Mehler, M.F., P.C. Mabie, G. Zhu, S. Gokhan, and J.A. Kessler. 2000. Developmental changes in progenitor cell responsiveness to bone

morphogenetic proteins differentially modulate progressive CNS lineage fate. *Dev. Neurosci.* 22:74–85. doi:10.1159/000017429

Miyawaki, T., A. Uemura, M. Dezawa, R.T. Yu, C. Ide, S. Nishikawa, Y. Honda, Y. Tanabe, and T. Tanabe. 2004. Tlx, an orphan nuclear receptor, regulates cell numbers and astrocyte development in the developing retina. *J. Neurosci.* 24:8124–8134. doi:10.1523/JNEUROSCI.2235-04.2004

Miyoshi, H., K.A. Smith, D.E. Mosier, I.M. Verma, and B.E. Torbett. 1999. Transduction of human CD34+ cells that mediate long-term engraftment of NOD/SCID mice by HIV vectors. *Science.* 283:682–686. doi:10.1126/science.283.5402.682

Mori, N., R. Stein, O. Sigmund, and D.J. Anderson. 1990. A cell type-preferred silencer element that controls the neural-specific expression of the SCG10 gene. *Neuron.* 4:583–594. doi:10.1016/0896-6273(90)90116-W

Morita, S., T. Kojima, and T. Kitamura. 2000. Plat-E: an efficient and stable system for transient packaging of retroviruses. *Gene Ther.* 7:1063–1066. doi:10.1038/sj.gt.3301206

Nakashima, K., S. Wiese, M. Yanagisawa, H. Arakawa, N. Kimura, T. Hisatsune, K. Yoshida, T. Kishimoto, M. Sendtner, and T. Taga. 1999a. Developmental requirement of gp130 signaling in neuronal survival and astrocyte differentiation. *J. Neurosci.* 19:5429–5434.

Nakashima, K., M. Yanagisawa, H. Arakawa, N. Kimura, T. Hisatsune, M. Kawabata, K. Miyazono, and T. Taga. 1999b. Synergistic signaling in fetal brain by STAT3-Smad1 complex bridged by p300. *Science.* 284:479–482. doi:10.1126/science.284.5413.479

Nakashima, K., T. Takizawa, W. Ochiai, M. Yanagisawa, T. Hisatsune, M. Nakafuku, K. Miyazono, T. Kishimoto, R. Kageyama, and T. Taga. 2001. BMP2-mediated alteration in the developmental pathway of fetal mouse brain cells from neurogenesis to astrocytogenesis. *Proc. Natl. Acad. Sci. USA.* 98:5868–5873. doi:10.1073/pnas.101109698

Namihira, M., J. Kohyama, K. Semi, T. Sanosaka, B. Deneen, T. Taga, and K. Nakashima. 2009. Committed neuronal precursors confer astrocytic potential on residual neural precursor cells. *Dev. Cell.* 16:245–255. doi:10.1016/j.devcel.2008.12.014

Nishihara, S., L. Tsuda, and T. Ogura. 2003. The canonical Wnt pathway directly regulates NRSF/REST expression in chick spinal cord. *Biochem. Biophys. Res. Commun.* 311:55–63. doi:10.1016/j.bbrc.2003.09.158

Olguín, P., P. Oteíza, E. Gamboa, J.L. Gómez-Skármeta, and M. Kukuljan. 2006. RE-1 silencer of transcription/neural restrictive silencer factor modulates ectodermal patterning during *Xenopus* development. *J. Neurosci.* 26:2820–2829. doi:10.1523/JNEUROSCI.5037-05.2006

Otto, S.J., S.R. McCorkle, J. Hover, C. Conaco, J.J. Han, S. Impey, G.S. Yochum, J.J. Dunn, R.H. Goodman, and G. Mandel. 2007. A new binding motif for the transcriptional repressor REST uncovers large gene networks devoted to neuronal functions. *J. Neurosci.* 27:6729–6739. doi:10.1523/JNEUROSCI.0091-07.2007

Rothstein, J.D., L. Martin, A.I. Levey, M. Dykes-Hoberg, L. Jin, D. Wu, N. Nash, and R.W. Kuncl. 1994. Localization of neuronal and glial glutamate transporters. *Neuron.* 13:713–725. doi:10.1016/0896-6273(94)90038-8

Schoenherr, C.J., A.J. Paquette, and D.J. Anderson. 1996. Identification of potential target genes for the neuron-restrictive silencer factor. *Proc. Natl. Acad. Sci. USA.* 93:9881–9886. doi:10.1073/pnas.93.18.9881

Schuurmans, C., and F. Guillemot. 2002. Molecular mechanisms underlying cell fate specification in the developing telencephalon. *Curr. Opin. Neurobiol.* 12:26–34. doi:10.1016/S0959-4388(02)00286-6

See, J., P. Mamontov, K. Ahn, L. Wine-Lee, E.B. Crenshaw III, and J.B. Grinspan. 2007. BMP signaling mutant mice exhibit glial cell maturation defects. *Mol. Cell. Neurosci.* 35:171–182. doi:10.1016/j.mcn.2007.02.012

Setoguchi, H., M. Namihira, J. Kohyama, H. Asano, T. Sanosaka, and K. Nakashima. 2006. Methyl-CpG binding proteins are involved in restricting differentiation plasticity in neurons. *J. Neurosci. Res.* 84:969–979. doi:10.1002/jnr.21001

Shi, Y., D. Chichung Lie, P. Taupin, K. Nakashima, J. Ray, R.T. Yu, F.H. Gage, and R.M. Evans. 2004. Expression and function of orphan nuclear receptor TLX in adult neural stem cells. *Nature.* 427:78–83. doi:10.1038/nature02211

Singh, S.K., M.N. Kagalwala, J. Parker-Thornburg, H. Adams, and S. Majumder. 2008. REST maintains self-renewal and pluripotency of embryonic stem cells. *Nature.* 453:223–227. doi:10.1038/nature06863

Song, H., C.F. Stevens, and F.H. Gage. 2002. Astroglia induce neurogenesis from adult neural stem cells. *Nature.* 417:39–44. doi:10.1038/417039a

Su, X., S. Kameoka, S. Lentz, and S. Majumder. 2004. Activation of REST/NRSF target genes in neural stem cells is sufficient to cause neuronal differentiation. *Mol. Cell. Biol.* 24:8018–8025. doi:10.1128/MCB.24.18.8018-8025.2004

Takizawa, T., K. Nakashima, M. Namihira, W. Ochiai, A. Uemura, M. Yanagisawa, N. Fujita, M. Nakao, and T. Taga. 2001. DNA methylation is a critical cell-intrinsic determinant of astrocyte differentiation in the fetal brain. *Dev. Cell.* 1:749–758. doi:10.1016/S1534-5807(01)00101-0

Temple, S. 2001. The development of neural stem cells. *Nature.* 414:112–117. doi:10.1038/35102174

Tokunaga, A., J. Kohyama, T. Yoshida, K. Nakao, K. Sawamoto, and H. Okano. 2004. Mapping spatio-temporal activation of Notch signaling during neurogenesis and gliogenesis in the developing mouse brain. *J. Neurochem.* 90:142–154. doi:10.1111/j.1471-4159.2004.02470.x

Uemura, A., S. Kusuhara, S.J. Wiegand, R.T. Yu, and S. Nishikawa. 2006. Tlx acts as a proangiogenic switch by regulating extracellular assembly of fibronectin matrices in retinal astrocytes. *J. Clin. Invest.* 116:369–377. doi:10.1172/JCI25964

Watanabe, Y., S. Kameoka, V. Gopalakrishnan, K.D. Aldape, Z.Z. Pan, F.F. Lang, and S. Majumder. 2004. Conversion of myoblasts to physiologically active neuronal phenotype. *Genes Dev.* 18:889–900. doi:10.1101/gad.1179004

Westbrook, T.F., G. Hu, X.L. Ang, P. Mulligan, N.N. Pavlova, A. Liang, Y. Leng, R. Maehr, Y. Shi, J.W. Harper, and S.J. Elledge. 2008. SCFbeta-TRCP controls oncogenic transformation and neural differentiation through REST degradation. *Nature.* 452:370–374. doi:10.1038/nature06780

Yanagisawa, M., K. Nakashima, T. Takizawa, W. Ochiai, H. Arakawa, and T. Taga. 2001. Signaling crosstalk underlying synergistic induction of astrocyte differentiation by BMPs and IL-6 family of cytokines. *FEBS Lett.* 489:139–143. doi:10.1016/S0014-5793(01)02095-6

Yoshiura, S., T. Ohtsuka, Y. Takenaka, H. Nagahara, K. Yoshikawa, and R. Kageyama. 2007. Ultradian oscillations of Stat, Smad, and Hes1 expression in response to serum. *Proc. Natl. Acad. Sci. USA.* 104:11292–11297. doi:10.1073/pnas.0701837104

Cell Stem Cell

Signaling through BMPR-IA Regulates Quiescence and Long-Term Activity of Neural Stem Cells in the Adult Hippocampus

Helena Mira,[1,2,10,*] Zoraida Andreu,[2,3,10] Hoonkyo Suh,[1,4] D. Chichung Lie,[5] Sebastian Jessberger,[1,6] Antonella Consiglio,[1,7] Juana San Emeterio,[2] Rafael Hortigüela,[2] María Ángeles Marqués-Torrejón,[3] Kinichi Nakashima,[1,8] Dilek Colak,[9] Magdalena Götz,[9] Isabel Fariñas,[3] and Fred H. Gage[1,*]

[1]Laboratory of Genetics, The Salk Institute for Biological Studies, La Jolla, CA 92037, USA
[2]Área de Biología Celular y Desarrollo, Centro Nacional de Microbiología, Instituto de Salud Carlos III, Majadahonda, 28220 Madrid, Spain
[3]Departament de Biologia Cellular, Universitat de València and CIBERNED, 46100 València, Spain
[4]Stem Cells and Regenerative Medicine, Lerner Research Institute, Cleveland Clinic, Cleveland, OH 44195, USA
[5]Institute for Developmental Genetics, Helmholtz Center Munich, German Research Center for Environmental Health, 85764 Munich-Neuherberg, Germany
[6]Institute of Cell Biology, Department of Biology, ETH Zurich, 8092 Zurich, Switzerland
[7]Centre de Medicina Regenerativa de Barcelona, 08003 Barcelona, Spain
[8]Laboratory of Molecular Neuroscience, Graduate School of Biological Sciences, Nara Institute of Science and Technology, 8916-5 Takayama, 630-0101 Ikoma, Japan
[9]Institute for Stem Cell Research, Helmholtz Center Munich, German Research Center for Environmental Health, 85764 Munich-Neuherberg, Germany
[10]These authors contributed equally to this work
*Correspondence: helena.mira@uv.es (H.M.), gage@salk.edu (F.H.G.)
DOI 10.1016/j.stem.2010.04.016

SUMMARY

Neural stem cells (NSCs) in the adult hippocampus divide infrequently, and the molecules that modulate their quiescence are largely unknown. Here, we show that bone morphogenetic protein (BMP) signaling is active in hippocampal NSCs, downstream of BMPR-IA. BMPs reversibly diminish proliferation of cultured NSCs while maintaining their undifferentiated state. In vivo, acute blockade of BMP signaling in the hippocampus by intracerebral infusion of Noggin first recruits quiescent NSCs into the cycle and increases neurogenesis; subsequently, it leads to decreased stem cell division and depletion of precursors and newborn neurons. Consistently, selective ablation of *Bmpr1a* in hippocampal NSCs, or inactivation of BMP canonical signaling in conditional *Smad4* knockout mice, transiently enhances proliferation but later leads to a reduced number of precursors, thereby limiting neuronal birth. BMPs are therefore required to balance NSC quiescence/proliferation and to prevent loss of the stem cell activity that supports continuous neurogenesis in the mature hippocampus.

INTRODUCTION

Quiescence of somatic stem cells is critically important for the maintenance of tissue-specific germinal reservoirs during adulthood. Stem cells from diverse adult compartments are depleted when forced to proliferate (Cheng et al., 2000; Kippin et al., 2005; Ruzankina et al., 2007), and quiescence may function as a protective mechanism that counteracts stem cell exhaustion. In the mature mammalian nervous system, adult neural stem cells (NSCs) generate new neurons throughout life, but there is little information regarding the molecules that regulate their relative quiescence. Adult NSCs are located in two specialized brain niches: the subependymal zone (SEZ), which lines the lateral ventricles, and the hippocampal subgranular zone (SGZ) apposed to the innermost layer of the dentate gyrus (reviewed by Temple and Alvarez-Buylla, 1999; Zhao et al., 2008). In the latter, undifferentiated cells expressing the Sry-related high mobility group (HMG) box transcription factor *Sox2* are the primary source for NSCs. On the basis of morphological criteria, on the expression of unique sets of cellular markers, and on lineage tracing, two types of lineage-related SOX2$^+$ stem/precursor cells that contribute neuronal progeny have been identified in the SGZ: (1) radial SOX2$^+$ cells, which bear a radial process spanning the granule cell layer and express NESTIN, the glutamate transporter GLAST, and the glial fibrillary acidic protein GFAP among other markers (also named rA cells or type 1 cells), and (2) nonradial SOX2$^+$ cells (or type 2a), which may arise from the radial cells and do not express GFAP. This distinction correlates with a different proliferation state of the cells, as SOX2$^+$ radial cells rarely divide whereas SOX2$^+$ nonradial cells appear to cycle relatively more often; consequently, it has been suggested that the radial cell population constitutes a stem cell reservoir (Seri et al., 2001, 2004; Filippov et al., 2003; Fukuda et al., 2003; Kronenberg et al., 2003; Suh et al., 2007).

Although the phenotypes of both radial and nonradial SOX2$^+$ cell types have been extensively characterized in numerous studies, our molecular understanding of their regulation is still very limited. In vivo cycling of the adult hippocampal SOX2$^+$

NSC population is relatively low, and most cells are held in a quiescent state. Indeed, in young transgenic mice harboring the green fluorescent protein (GFP) under the control of the murine *Sox2* promoter, less than 10% of the *Sox2*-GFP$^+$ cells in the SGZ colabel with cell proliferation markers (Suh et al., 2007). As rodents grow old (Hattiangady and Shetty, 2008; Aizawa et al., 2009), SOX2$^+$ cells lose proliferative capacity, suggesting that adult NSCs may have a finite number of cycles. This finding points to a role for quiescence in the maintenance of the regenerative potential of the hippocampal dentate gyrus. However, how quiescence of SOX2$^+$ stem cells is governed during adulthood is still an unresolved question.

Among the signaling pathways that govern stem cells across phylogeny, bone morphogenetic proteins (BMPs) have emerged as critical regulators of stem cell self-renewing divisions and maintenance in a wide variety of niches (reviewed by Varga and Wrana, 2005; Morrison and Spradling, 2008). BMPs belong to the TGF-β superfamily of cytokines and are pleiotropic molecules that exert a plethora of effects in the nervous system, ranging from dorsoventral patterning of the embryonic neural tube to proliferation, apoptosis, neurogenesis, and gliogenesis (reviewed by Panchision and McKay, 2002; Hall and Miller, 2004; Chen and Panchision, 2007). In the adult brain environment, the contribution of BMP signaling to stem cell regulation remains largely unexplored, although recently it has been suggested that the BMP pathway may have a central role in modulating NSC function (Lim et al., 2000; Coskun et al., 2001; Colak et al., 2008; Bonaguidi et al., 2008).

Here, we test the requirement of endogenous BMP signaling for the regulation of hippocampal NSCs. Both genetic deletion of *Bmpr1a* and *Smad4* in adult NSCs and infusion of the BMP antagonist Noggin show that canonical signaling downstream of the BMP type IA receptor is a key mediator of quiescence in adult NSCs. We evaluate BMP function both in vitro and in vivo and conclude that BMPR-IA is essential in regulating the equilibrium between stem cell proliferation and quiescence in the SGZ, preventing the premature depletion of NSC activity in the mature hippocampus.

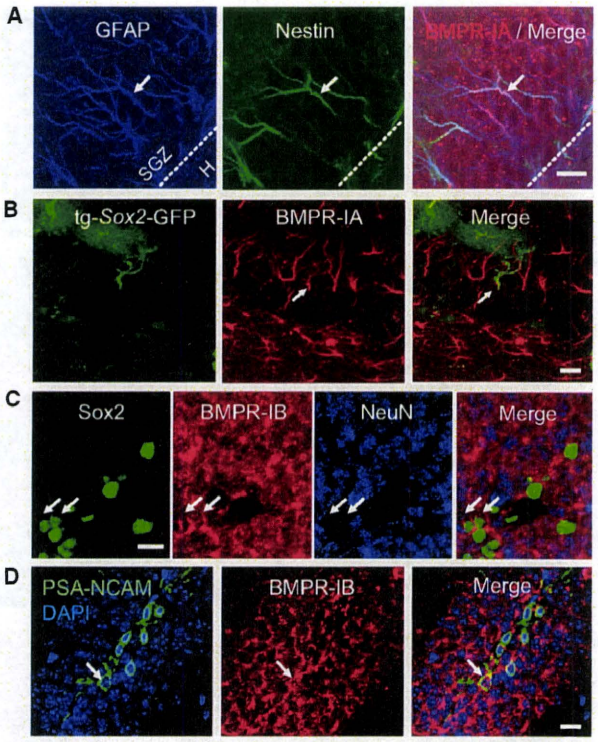

Figure 1. Adult Hippocampal Radial Stem Cells Express BMPR-IA

(A) Confocal microscopy images of adult hippocampal mouse sections showing GFAP (blue), NESTIN (green), and BMPR-IA (red) triple-labeled processes (arrow) of NSCs projecting radially from the SGZ (dotted line). See also Figure S1 for additional data. The scale bar represents 20 μm.

(B) Section from an adult tg-*Sox2*-GFP mouse. Arrow points to a radial stem cell process (immunoreactive for GFP, green) labeled for BMPR-IA (red). The scale bar represents 20 μm.

(C) BMPR-IB staining was detected in NeuN$^+$ granule neurons located in the granule cell layer and in some SOX2$^+$ cells (arrows) located in the SGZ. The scale bar represents 10 μm.

(D) Immature neurons expressing PSA-NCAM also stained for BMPR-IB. The scale bar represents 20 μm. H, hilus. See scheme in Figure S7.

RESULTS

BMPR-IA Is Expressed by Adult Hippocampal Radial NSCs

BMP ligands signal through a tetrameric complex formed by the BMP type II receptor (BMPR-II) and different classes of BMP type I receptors, the prototypic ones being BMPR-IA (ALK3) and BMPR-IB (ALK6). Expression of *Bmpr-II* had been previously documented in the hippocampus by in situ hybridization (Söderström et al., 1996; Charytoniuk et al., 2000), so we analyzed type I receptor expression by immunostaining. We found that radial stem cells coexpressing GFAP and NESTIN were frequently stained for BMPR-IA (Figure 1A). Consistently, BMPR-IA signal was detected in GFP$^+$ radial cells from transgenic mice expressing the GFP reporter under the regulation of the *Sox2* promoter (Figure 1B). In addition, the vast majority of GFAP$^+$ astrocytes in the dentate gyrus and the hilar region were immunoreactive for BMPR-IA (Figure 1A and Figure S1, available online). In marked contrast, BMPR-IB expression was mostly confined to the neuronal population, given that NeuN$^+$ mature neurons and PSA-NCAM$^+$ immature neurons stained for BMPR-IB (Figures 1C and 1D). Some nonradial cells that formed clusters in the SGZ expressed low levels of SOX2 and were also immunoreactive for BMPR-IB (Figure 1C). Altogether, these findings suggested that BMPR-IA might regulate an early event in adult neurogenesis, whereas BMPR-IB might have a later role, during neuronal differentiation.

Canonical BMP Signaling in the Adult Hippocampus Is Active in Nondividing SGZ Cells

The interaction of BMPs with their receptors can trigger several pathways, including the "canonical" Smad-mediated pathway, in which activated BMPR-I phosphorylates the DNA binding proteins SMAD1/5/8, causing their nuclear translocation. Immunostaining with anti-phospho-SMAD1 (Ser463/465) was assessed in adult animals that were briefly pulsed with the S-phase marker 5-bromodeoxyuridine (BrdU). P-SMAD1 staining revealed that canonical BMP signaling is active in the majority of radial and

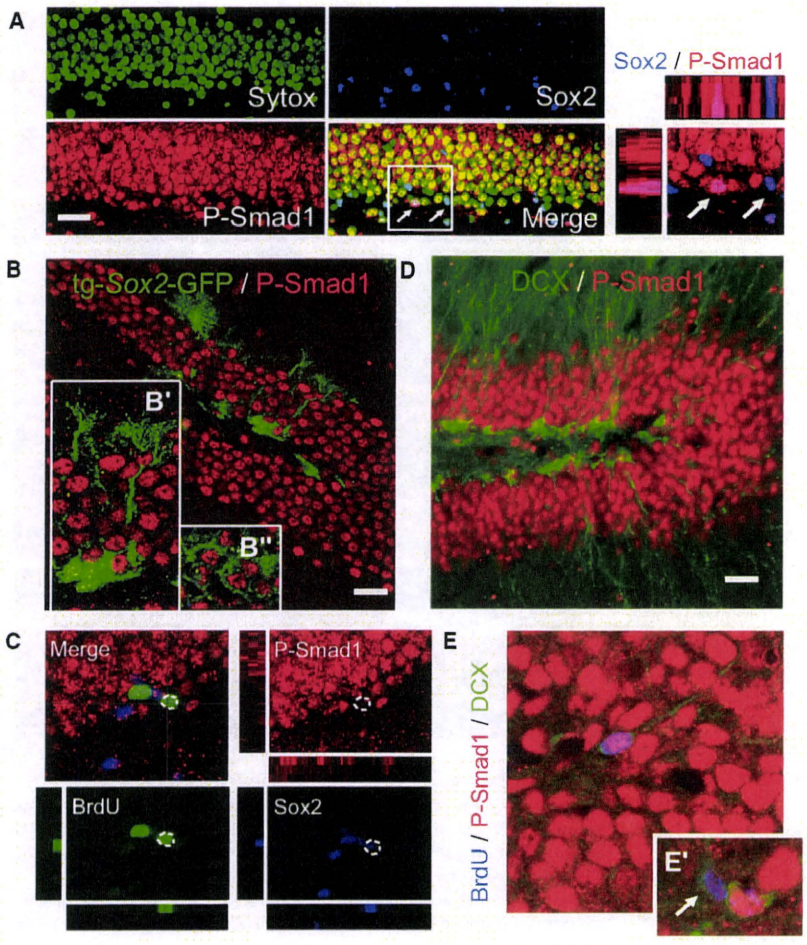

Figure 2. BMP Signaling Is Active in Adult Hippocampal Stem/Precursor Cells that Are Not Cycling

(A) Confocal microscopy images of adult hippocampal mouse sections showing that most SOX2$^+$ cells (blue) in the SGZ are immunoreactive for P-SMAD1 (red) in their nucleus (green; fraction of SOX2$^+$ cells that were P-SMAD1$^+$: 64% ± 1%, average ± SEM, n = 2). Of these, ~70% displayed medium to high signal level. Confocal 3D reconstruction of the boxed area, showing colocalization of phosphorylated SMAD1 and SOX2 proteins in some SGZ nuclei (left arrow), is shown on the right. Top shows the *x-z* plane; left shows the *y-z* plane. The scale bar represents 40 μm.

(B) Image of a section from a tg-*Sox2*-GFP transgenic mouse showing the P-SMAD1$^+$ nucleus of radial (B′) and nonradial (B″) *Sox2*-expressing NSCs (immunoreactive for GFP, green). The scale bar represents 40 μm.

(C) Section from an adult animal pulsed with BrdU (four injections every 2 hr) and euthanized 1 hr later. The immunostaining and the confocal analysis shows SOX2$^+$ cells that incorporated BrdU and were negative for P-SMAD1 (dotted circles).

(D) Most DCX$^+$ immature neurons (green) in the SGZ stained for P-SMAD1. Note that nuclei of densely packed mature neurons located in the granule layer were also immunoreactive for P-SMAD1. The scale bar represents 40 μm.

(E) Detail from a section of an adult animal labeled with BrdU, showing a newborn neuron (DCX$^+$BrdU$^+$) that stained for P-SMAD1 apparently migrating into the granule layer. As shown in (E′), we could observe some newborn neurons with poor dendritic processes that did not stain for P-SMAD1 (arrow). See also Figure S2 for additional data. See scheme in Figure S7.

nonradial SOX2$^+$ cells (Figures 2A and 2B), but the pathway is preferentially inactive in the few cells that have entered a new round of cell division (most SOX2$^+$ cells that incorporated BrdU were negative for P-SMAD1: 92% ± 8%, average ± SEM, Figure 2C). In addition, the majority of the doublecortin-positive (DCX$^+$) and NEUROD1$^+$ immature neurons/neuroblasts stained for P-SMAD1 (Figure 2D and Figure S2). When adult animals were pulsed with BrdU for 3 days for labeling and tracking newborn cells, we observed that most of the DCX$^+$BrdU$^+$ newly generated neurons that were extending dendritic processes toward the molecular layer were P-SMAD1$^+$ (Figure 2E); however, we also found some more immature DCX$^+$BrdU$^+$ cells positioned along the SGZ, with shorter dendrites, that were negative for P-SMAD1 (Figure 2E′), suggesting that canonical signaling becomes reactivated in the neuronal progeny shortly after its commitment. Together, our results indicated that BMP signaling is inactive in most proliferating SGZ cells, whereas it is active in nondividing cells, including the quiescent SOX2$^+$ NSC population and the differentiated neurons.

BMP2/4 Trigger Canonical Signaling in Adult Hippocampal NSC Cultures Expressing BMPR-IA

We next examined the role of BMP signaling in adult hippocampus-derived NSCs (AH-NSCs) that can mimic the initial events of neurogenesis under proliferating conditions. Immunostaining and RT-PCR analysis revealed that AH-NSCs expressed *Bmpr1a* and *Bmpr2*, whereas *Bmpr1b* expression was only detected at very weak levels (Figures 3A and 3B). Of note, *Bmpr1a* expression was decreased, whereas *Bmpr1b* expression was progressively increased upon neuronal differentiation of AH-NSCs (Figure S3). Given that BMPR-IA preferentially binds ligands from the Dpp class (BMP2/4) as opposed to the 60A class (BMP5-8) (ten Dijke et al., 1994), we challenged AH-NSCs with the purified recombinant BMP2 and BMP4 proteins. BMP2/4 triggered phosphorylation and nuclear translocation of SMAD1 (Figures 3C and 3D) and upregulated the expression of several SMAD targets, such as *Id1-4*, *Hes1*, or the inhibitory *Smad6/7* genes (Figures 3E and 3F), showing that AH-NSCs responded to BMPs through activation of the canonical pathway.

BMP2/4 Treatment Decreases Proliferation and Increases Quiescence of AH-NSC Cultures

We assayed for proliferation effects of BMPs in AH-NSCs grown under self-renewing conditions in the presence of fibroblast growth factor 2 (FGF2). Under mitogenic stimulation, exposure to increasing BMP2 doses markedly decreased the percentage of cells that incorporated BrdU ($p < 0.05$, Figures 4A and 4B).

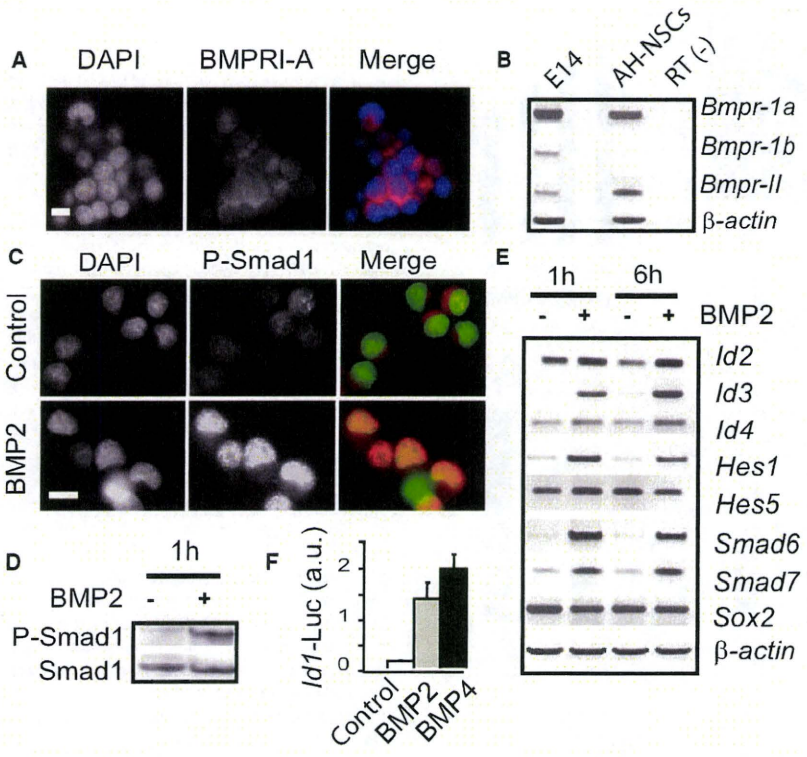

Figure 3. BMP Treatment Activates Canonical Signaling in AH-NSC Cultures Expressing BMPR-IA

(A) Immunofluorescent microscopy image showing BMPR-IA signal in AH-NSCs, growing in the presence of FGF2. The scale bar represents 10 μm.

(B) *Bmpr-1a* and *Bmpr-II* are expressed in proliferating AH-NSC cultures, as detected by RT-PCR. *Bmpr-1b* expression is low (average threshold cycle calculated by real-time quantitative RT-PCR [Cp ± SEM]: 28.4 ± 0.3 for *Bmpr-1a* and 31.0 ± 0.1 for *Bmpr-1b*). See also Figure S3 for additional data.

(C) Immunofluorescent analysis of BMP2-treated and untreated AH-NSCs, showing activation of canonical BMP signaling through increased phosphorylation and nuclear translocation of SMAD1. The scale bar represents 10 μm.

(D) Western blot analysis of protein extracts from BMP2-treated and untreated AH-NSCs corroborating the activation of canonical signaling through phosphorylation of SMAD1.

(E) mRNA expression of several SMAD target genes by RT-PCR.

(F) Relative luciferase activity in AH-NSCs electroporated with *Id1*-reporter construct upon BMP2/BMP4 stimulation.

Consistently, cell cycle analysis by flow cytometry indicated that BMP treatment increased the proportion of cells in G_0/G_1 while decreasing the proportion of AH-NSCs in S phase and G_2/M phases (Figure S4). The decrease in proliferation was not due to cell death (propidium iodide labeled cells by flow cytometry: 1.26% ± 0.43% in FGF2 versus 0.95% ± 0.06% in FGF2+BMP4, $p = 0.28$) or to differentiation, given that the expression of the NSC marker SOX2 was maintained in the culture (Figure 4A). Rather, BMP appeared to antagonize the proliferative function of FGF2 because increasing the amount of mitogen in the medium partially blocked the dose-dependent effect of the BMP treatment on proliferation (Figure S5; Pera et al., 2003).

We next explored whether BMP treatment increased the quiescent (G_0-arrested) cell fraction. Given that G_0 cells are in a lower metabolic state and do not require robust RNA transcription, they can be identified by a 2N DNA content and a low level of RNA, with Hoechst 33342 and the Pyronin Y RNA dye. Two-parameter flow cytometry showed that the fraction of G_0 cells increased an average fold of 1.8 ± 0.2 after BMP exposure ($n = 3$, Figure S4). Moreover, when the BMP-treated FACS-sorted G_0 cells were challenged with the BMP antagonist Noggin, 81.3% ± 10.7% of the cells were NESTIN$^+$ (not shown) and 21.6% ± 7.8% of the cells started dividing after 24–48 hr (Figure S4). This finding indicated that the majority of the BMP-treated G_0 cells maintained stem/precursor properties and could re-enter the cell cycle. Thus, Noggin reverted the G_0 arrest induced by BMP signaling on AH-NSCs.

To test whether culture conditions such as cell density and adhesion influenced BMP functions, we also assayed for the effects of BMPs on AH-NSCs seeded at a very low density (0.5 cells/μL) and maintained as clonal floating aggregates termed neurospheres. Comparable numbers of spheres were formed in control medium with FGF2 or in medium containing FGF2 and 50 ng/mL BMP2/4 (331.67 ± 49.14 spheres in FGF2 versus 323.50 ± 83.19 spheres in FGF2+BMP4, $p = 0.46$, Figure 4C). We evaluated the proportion of cells per sphere that were in the cell cycle, using an antibody directed against Ki67, a protein that is present during all active phases of the cell cycle but is absent from resting (G_0) cells. The percentage of Ki67$^+$ cells was markedly diminished in the presence of BMP4 ($p < 0.05$, Figures 4E and 4F), and accordingly, the average diameter of the spheres was significantly decreased ($p < 0.05$, Figures 4C and 4D). Consistent with our previous results, cell death was unaffected (percentage of Caspase3$^+$ cells per sphere: 0.64% ± 0.46% in FGF2 versus 1.22 ± 0.3% in FGF2+BMP4, $p = 0.29$), and the proportion of cells that were NESTIN$^+$ or SOX2$^+$ did not change (Figure 4E, percentage of NESTIN$^+$ cells per neurosphere: 83.65% ± 3.74% in FGF2 versus 97.72% ± 1.85% in FGF2+BMP4; percentage of SOX2$^+$ cells: 89.27% ± 0.64% in FGF2 versus 92.6 ± 0.57% in FGF2+BMP4). In addition, >80% of the Ki67$^-$ cells were immunoreactive for NESTIN and SOX2, indicating that, at early time points, most G_0 (Ki67$^-$) cells were undifferentiated/immature and not terminally differentiated cells (Figure S5). Nevertheless, ~20% of the Ki67$^-$ cells expressed differentiation markers of the oligodendroglial or astroglial lineage, but no significant differences were found between control and BMP-treated neurospheres.

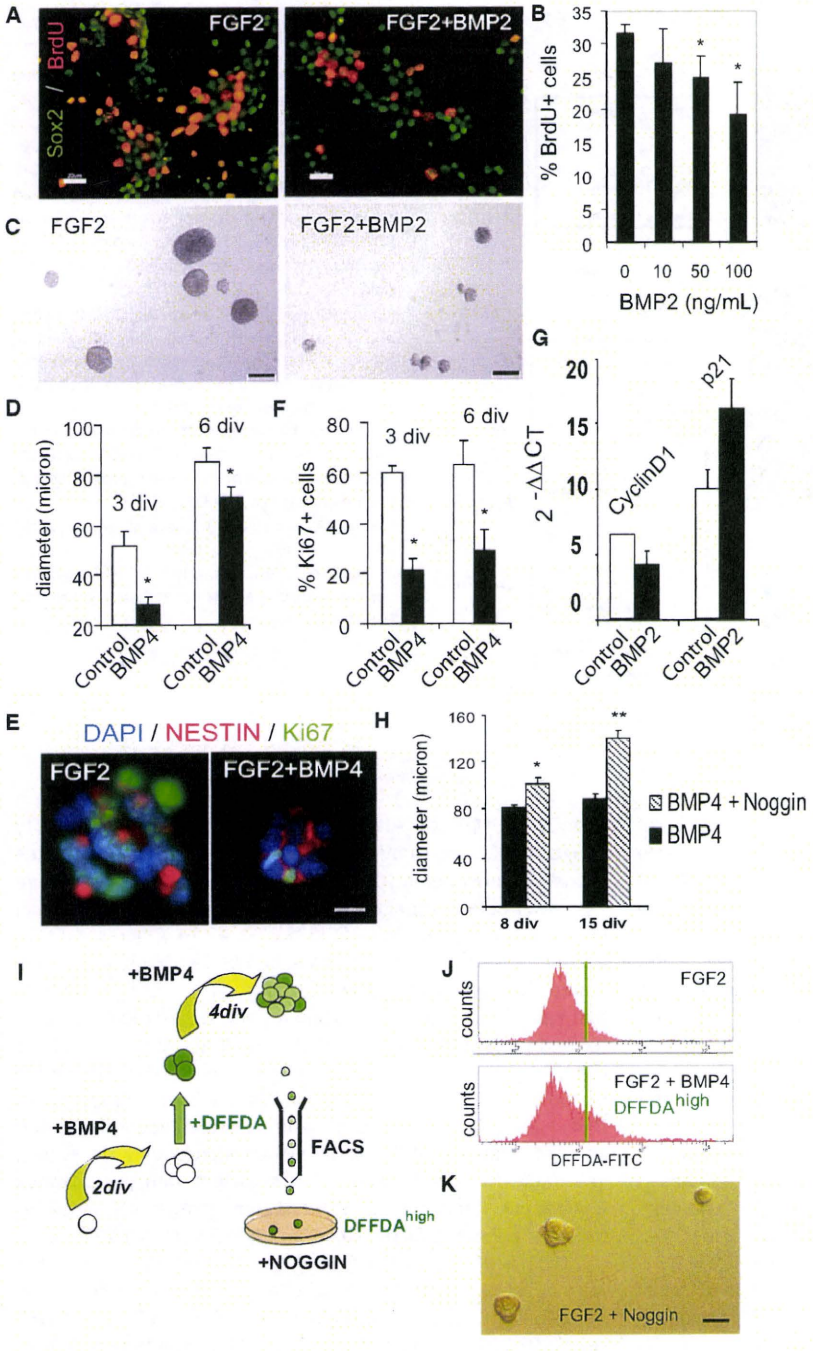

Figure 4. BMP Treatment Decreases Proliferation and Increases Quiescence of AH-NSC Cultures

(A) Immunofluorescent analysis of BMP-treated or untreated proliferating cells fixed at 2 days in vitro. BMP2 decreases the proportion of cells that are in S-phase ($BrdU^+$, red) while maintaining the expression of the NSC marker SOX2 (green). Scale bars represent 20 μm.

(B) Quantitative analysis showing that increasing concentrations of BMP2 decrease the percentage of $BrdU^+$ cells in AH-NSC cultures grown in proliferating medium with FGF2 (n = 3).

(C) Bright-field images of adult hippocampal neurospheres grown for 6 days in vitro. Note that approximately equal numbers of neurospheres are generated in the presence or absence of BMP2; however, the decrease in sphere size in BMP2-treated cultures is apparent. The scale bar represents 100 μm.

(D) A plot of the diameter of spheres that were generated after plating AH-NSCs in nonadherent conditions at very low density (250 viable cells per cm^2, n = 3).

(E) Immunofluorescent analysis of BMP-treated or untreated neurospheres fixed at 3 days in vitro. BMP4 decreases the proportion of cells that are in the cell cycle ($Ki67^+$, green) while maintaining the expression of the NSC marker NESTIN (red). The scale bar represents 10 μm.

(F) BMP4 treatment decreases the percentage of $Ki67^+$ cells per neurosphere (n = 3).

(G) qRT-PCR analysis showing decreased *CyclinD1* and increased $p21^{cip1/waf1}$ expression 4 days after BMP2 treatment of adult hippocampal sphere cultures (n = 2).

(H) The addition of Noggin (250 ng/mL) at day 6 progressively rescues the proliferating activity (size) of the BMP-treated spheres, as measured at days 8 and 15.

(I) Diagram depicting the experimental design employed to purify DFFDA-retaining cells from BMP4-treated neurospheres.

(J) Cytometry plot showing that BMP4 treatment increased the percentage of $DFFDA^{high}$ cells from 11% to 27%.

(K) Bright-field image of purified BMP4-treated $DFFDA^{high}$ cells plated in FGF2 + Noggin (100 ng/mL), showing secondary sphere formation after 48 hr. Paired Student's t test relative to control condition: $^*p < 0.05$, $^{**}p < 0.01$. The scale bar represents 20 mm. See also Figures S4 and S5 for additional data.

The decreased proliferation and increased G_0 cell fraction after BMP exposure correlated with the upregulation of the cell cycle inhibitor *Cdkn1a* ($p21^{Cip1/Waf1}$) and the downregulation of *CyclinD1* (Figure 4G). In addition, Noggin treatment in the presence of FGF2 presumably antagonized endogenous BMP effects by increasing the average sphere number (126% ± 4%) and diameter (187% ± 27%) and the percentage of $Ki67^+$ cells (120% ± 9%). Moreover, in agreement with a previous report (Bonaguidi et al., 2008), Noggin enhanced the net expansion of hippocampal sphere cultures that were serially passaged over 1 month in the presence of FGF2 but was not sufficient to promote proliferation of AH-NSCs (Figure S5).

At the level of clone size, the antiproliferative effect of BMP signaling could be reversed when BMP was replaced with

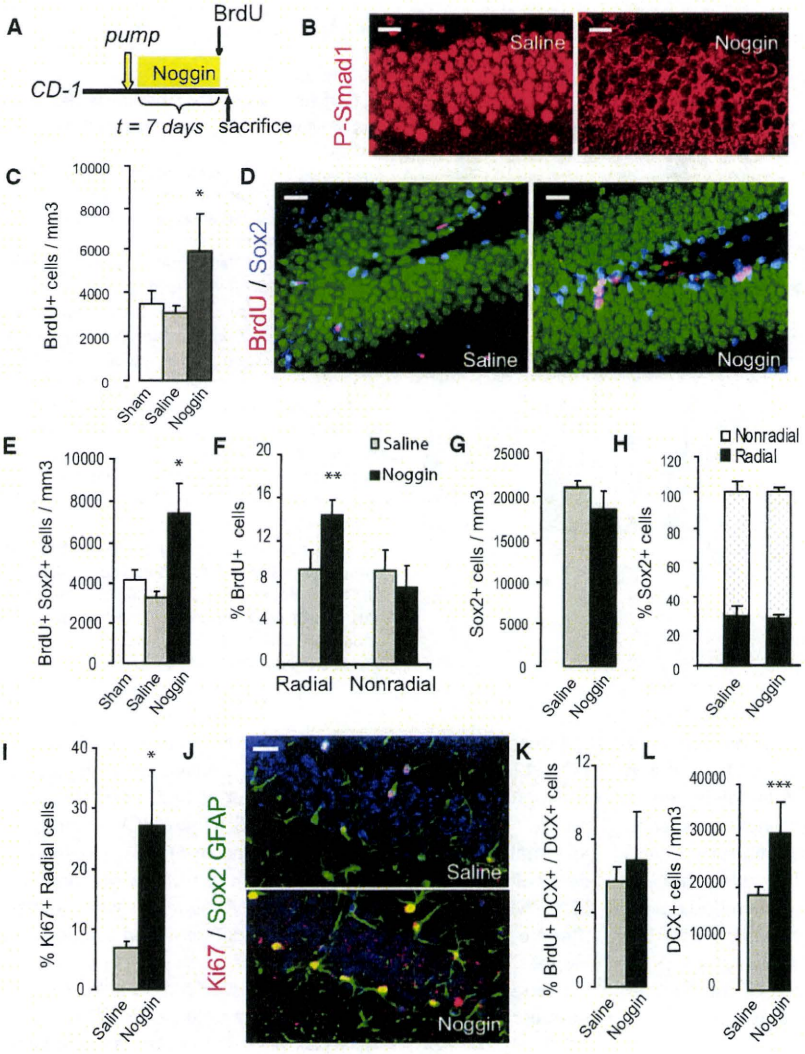

Figure 5. In Vivo Infusion of Noggin Increases Proliferation of SOX2$^+$ Radial NSCs

(A) Diagram depicting the experimental design employed. BrdU (seven injections every 2 hours) was administered prior to euthanasia.

(B) P-SMAD1 immunostaining in hippocampal sections from saline- and Noggin-infused mice. Note that nuclear localization of P-SMAD1 is abolished after Noggin exposure, demonstrating that the treatment was effective. Scale bars represent 20 μm.

(C) Quantitative analysis showing that 1 week of Noggin infusion enhanced cell proliferation in the hippocampus. Proliferation was calculated by the number of cells that incorporated BrdU per volume of granule cell layer.

(D) Confocal microscopy images of adult hippocampal mouse sections showing the increase in proliferative NSCs double labeled for SOX2 (blue) and BrdU (red). Nuclei were stained with Sytox-Green. Scale bars represent 40 μm.

(E) Immediately after 1 week of Noggin delivery, the number of SOX2$^+$ cells in S-phase increased.

(F) The percentage of radial cells (immunoreactive for SOX2 and GFAP) that incorporated BrdU increased; the proportion of nonradial cells (immunoreactive for SOX2 but not for GFAP) that incorporated BrdU did not change.

(G) The total number of SOX2$^+$ cells per volume of granule cell layer remained constant.

(H) The relative amount of radial and nonradial cells was maintained.

(I) Noggin increased the percentage of radial SOX2$^+$ cells that are in the cell cycle (Ki67$^+$).

(J) Confocal image showing that Noggin increased cell cycle entry of the radial NSC population. The scale bar represents 40 μm.

(K and L) The rate of proliferation of doublecortin-expressing (DCX$^+$) neuroblasts did not change (K), although as shown in (L), the total number of DCX$^+$ immature neurons augmented. Unpaired Student's t test: $^*p < 0.05$, $^{**}p < 0.01$, and $^{***}p < 0.001$.

Noggin (see the recovery of sphere diameters, Figure 4H). We confirmed this reversibility at the cellular level, by using the cytoplasmic retention dye carboxy-DFFDA, which is subject to dilution upon cell division. As illustrated in Figure 4I, we loaded spheres that were growing for 2 days with DFFDA, and we allowed them to grow for 4 additional days in FGF2+BMP4. Addition of BMP4 clearly increased (~2.5-fold) the DFFDA^{high} cell fraction (nondividing cells) relative to the control condition (Figure 4J). When BMP-treated DFFDA^{high} cells were FACS sorted and were placed at low density in FGF2 + Noggin medium, 46% ± 20% of the cells re-entered the cell cycle (were Ki67$^+$) and 35% ± 16% formed secondary clones (Figure 4K). These results collectively indicated that BMPs counteract the mitogenic stimulation of AH-NSCs by promoting the entry of the cells into quiescence. The contribution of other BMP signaling effects (i.e., cell cycle lengthening effects) to the decrease in proliferation cannot be excluded and remain to be explored.

BMP Signaling Regulates the Balance between AH-NSC Proliferation and Quiescence In Vivo

To assess the possibility that endogenous BMPs can regulate proliferation of NSCs in the hippocampal niche, we delivered Noggin into the lateral ventricle of the adult mouse brain. Animals were infused over 1 week and, on the last day of infusion, dividing cells were labeled with BrdU (Figure 5A). Acute delivery of Noggin efficiently blocked BMP canonical signaling in the hippocampus (Figure 5B) and increased the number of BrdU$^+$ cells in the SGZ (3073 ± 283 in saline [n = 8] versus 5868 ± 1853 in Noggin [n = 4], $p < 0.05$, Figure 5C).

Noggin infusion enhanced by 2-fold the percentage of SOX2$^+$ cells that were in S phase ($p < 0.05$, Figure 5D and 5E) but did not influence the total number of SOX2$^+$ cells in the SGZ ($p = 0.335$, Figure 5G) or the relative proportion of radial and nonradial cells (Figure 5H), suggesting that SOX2$^+$ cells divided asymmetrically. Interestingly, Noggin preferentially increased the proliferation of the GFAP$^+$SOX2$^+$ radial stem cell population ($p < 0.01$,

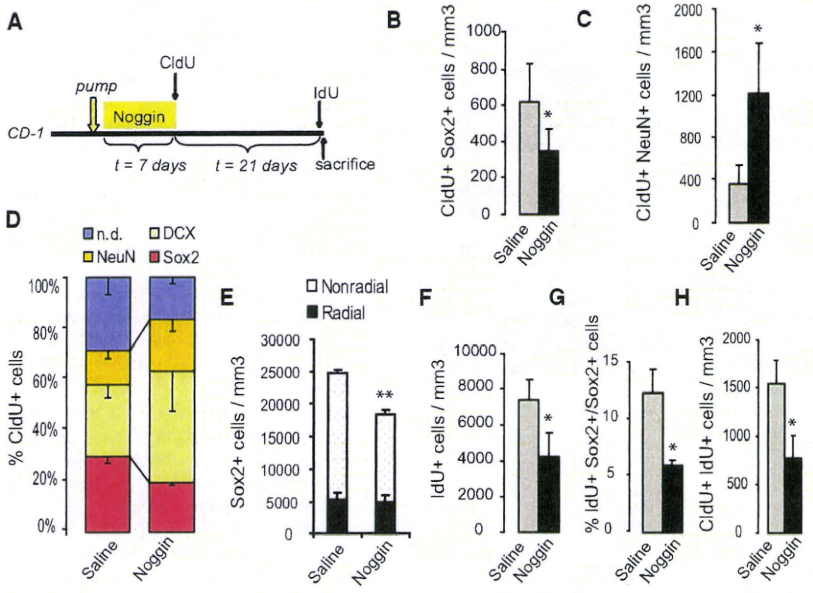

Figure 6. Noggin Infusion Leads in the Long Run to a Decrease in the Proliferative Activity of SOX2$^+$ Cells and of Label-Retaining NSCs

(A) Diagram depicting the experimental design for Noggin infusion and for the administration of CldU and IdU.

(B) Quantitative analysis showing that the number of SOX2$^+$ cells that retain the proliferative label CldU per volume of granule cell layer is decreased 3 weeks after pump removal.

(C) The number of NeuN$^+$ mature granule neurons marked with CldU is increased.

(D) The percentage of CldU$^+$ cells that stained for immature (DCX) and mature (NeuN) neuronal markers is increased at the expense of SOX2$^+$ cells. (n.d., not determined).

(E) The total number of SOX2$^+$ cells and the number of SOX2$^+$ nonradial cells per volume of granule cell layer decayed.

(F) Noggin exposure resulted 3 weeks later in decreased hippocampal proliferation (decreased number of IdU$^+$ cells/mm^3).

(G) Noggin exposure resulted in a reduction in the proportion of SOX2$^+$ cells undergoing cell division.

(H) The number of CldU$^+$LRCs that were still proliferating (incorporated IdU) was diminished. Unpaired Student's t test: *$p < 0.05$, **$p < 0.01$. See also Figure S6 for additional data.

Figure 5F), whereas the proportion of proliferating nonradial cells (Figure 5F) or DCX$^+$ neuroblasts remained constant (percentage of DCX$^+$ cells that were BrdU$^+$: 5.4% ± 0.7% in saline versus 6.9 ± 2.6% in Noggin, $p = 0.3$, Figure 5K). Immunofluorescence analysis with Ki67 further showed that the percentage of cycling radial NSCs increased (Figures 5I and 5J), indicating that the Noggin-mediated attenuation of BMP signaling recruited quiescent (G_0) radial cells into the cycle. In accordance with the increase in NSC division, hippocampal neurogenesis was augmented upon Noggin administration, as scored by the number of DCX$^+$ immature neurons ($p < 0.001$, Figure 5L).

Blockade of BMP Signaling Leads to a Decrease in Proliferation and to the Loss of SOX2$^+$ Nonradial Cells

In another set of animals, Noggin infusion was combined with the administration of two halogenated thymidine analogs to label and distinguish proliferating cells at different time points (Figure 6A). Noggin was administered over 1 week, and 5-clorodeoxyuridine (CldU) was injected on the last day of infusion (day 7). Next, the catheter connecting the pump to the cannula was sealed, and animals were returned to the cages for 3 additional weeks. Prior to euthanasia, animals received 5-iododeoxyuridine (IdU), which allowed us to discriminate between CldU$^+$ label-retaining stem cells (LRCs) that remained in the SGZ after the proliferative burst triggered by Noggin and IdU$^+$ cells that were dividing 28 days after they were first exposed to the BMP antagonist.

At least two major classes of cells in the hippocampal dentate gyrus were expected to retain the CldU label: slowly dividing SOX2$^+$ NSCs that do not dilute CldU through division (LRCs) and newborn neurons that incorporate CldU prior to cell cycle exit. As shown in Figure 6B, the number of SOX2$^+$CldU$^+$ LRCs per mm^3 in the SGZ was significantly reduced in brains that had been exposed to Noggin (619 ± 209 in saline [n = 5] versus 342 ± 124 in Noggin [n = 3], $p < 0.05$). Conversely, Noggin infusion significantly increased the number of CldU$^+$ cells that had matured to granule neurons ($p < 0.05$, Figure 6C). Among the cells that retained CldU, the proportion of SOX2$^+$ undifferentiated cells and that of their differentiated progeny (immature DCX$^+$ neurons or more mature NeuN$^+$ neurons) were shifted after Noggin infusion in favor of the differentiated phenotypes (Figure 6D).

In Noggin-treated animals, we observed that total SOX2$^+$ cell numbers were diminished because of a reduction in SOX2$^+$ nonradial cells ($p < 0.01$, Figure 6E). Accordingly, and as measured by anti-IdU immunostaining, overall proliferation in the SGZ was also diminished ($p < 0.05$, Figure 6F). The percentage of the SOX2$^+$ cell population that was in S-phase declined ($p < 0.05$, Figure 6G), the birth of new IdU$^+$DCX$^+$ neurons showed a marked tendency toward reduction (double-positive cells per mm^3: 4446 ± 729 in saline versus 2596 ± 702 in Noggin, $p = 0.09$), and the total number of DCX$^+$ cells per mm^3 was significantly diminished (21417 ± 2844 in saline versus 14785 ± 4134 in Noggin, $p < 0.05$). Of note, the number of double-labeled CldU$^+$IdU$^+$ cells in the SGZ decreased in the Noggin group compared to the saline condition ($p < 0.05$, Figure 6H), pointing to a restriction in the proliferative activity of LRCs.

To test the possibility that the loss of nonradial SOX2$^+$ cells was due to cell death, we examined the hippocampus at intermediate time points after Noggin infusion (Figure S6). Despite the progressive decline in the number of SOX2$^+$ nonradial cells, we could not detect any increase in the number of cleaved Caspase 3$^+$ nuclei in the SGZ. Thus, the cellular loss among the SOX2$^+$ nonradial pool was probably due to a decreased production of SOX2$^+$ nonradial cells but not to enhanced cell death.

BMPR-IA and Smad4 Are Required for Maintaining AH-NSC Activity and Neurogenesis In Vivo

We next designed a cell type- and time-specific strategy to accurately examine the role of canonical BMP signaling downstream of BMPR-IA in the regulation of AH-NSCs. We developed a lentivirus (LV)-mediated knockout technique to selectively delete *Bmpr1a* in *Sox2*-expressing cells (Figure 7A). *Bmpr1a*$^{flox/null}$ mice were stereotactically injected into the dentate gyrus with a LV expressing Cre recombinase fused to GFP under the regulation of the *Sox2* promoter (LV-*Sox2*-CreGFP). As a control, *Bmpr1a*$^{flox/wt}$ and *Bmpr1a*$^{flox/null}$ mice were injected with LV-*Sox2*-CreGFP or LV-*Sox2*-GFP, respectively. Animals received BrdU either 10 days or 4 weeks after LV injection. Among the LV-infected cells (GFP$^+$), the percentage of P-SMAD1$^+$ cells declined from 74.6% ± 5.7% (average ± SEM) in control mice to 38.5% ± 7.7% in *Bmpr1a*$^{flox/null}$ *mice*, indicating that canonical signaling was impaired. Ten days after *Bmpr1a* deletion, proliferation was increased in the SGZ, although high experimental variability and a local inflammatory response were observed. To analyze long-term effects of conditional *Bmpr1a* deletion in NSCs, we examined animals 28 days after LV injection. At this late time point, proliferation was markedly decreased (57% reduction, $p < 0.05$, Figures 7C and 7D), which is in accordance to our previous observations. Consistent with this finding, the total number of SGZ SOX2$^+$ cells was 51% lower ($p < 0.05$, Figures 7D and 7E), and the number of DCX$^+$ immature neurons was strongly reduced ($p < 0.05$, Figures 7D and 7F), indicating that neurogenesis was severely impaired upon deletion of *Bmpr1a*.

We next used a genetic approach to conditionally delete *Smad4*, a central player of the canonical BMP pathway, in the radial NSC population. We took advantage of the *GLAST:CreERT2* mouse line that expresses the tamoxifen-inducible form of Cre in adult NSCs (Ninkovic et al., 2007). *GLAST:CreERT2* animals were crossed with the *Smad4*$^{flox/flox}$ mouse line, and after tamoxifen-induced deletion of *Smad4*, dividing cells were labeled by means of BrdU. Animals were examined either immediately after or 3 weeks later (Figure 7G). We observed an increase in BrdU incorporation in the SGZ of conditionally deleted *Smad4* mice that were analyzed at short time points (BrdU$^+$ cells per mm^3: 751 ± 213 in *Smad4*$^{wt/wt}$ *versus* 1733 ± 47 in *Smad4*$^{flox/flox}$, $p < 0.05$, Figure 7H), yet when mice were examined 3 weeks later, we observed a reduction in SOX2$^+$ cell numbers, which was attributed to a decrease in non-radial cells (Figures 7I and 7J). This finding is in accordance with our previous data and clearly indicates that *Bmpr1a* and *Smad4* are involved in regulating the activity and the number of stem/precursor cells in the adult SGZ.

Our results demonstrate that canonical BMP signaling downstream of the BMP type IA receptor plays a key role in vivo in regulating quiescence of radial NSCs, which is required to maintain the proliferative capacity of the hippocampal stem cell pool and thus to support continuous neurogenesis throughout the adult life.

DISCUSSION

Interactions between neurogenic niches and NSCs play a critical role in the homeostatic regulation of adult neurogenesis. Signaling from the niche is proposed to control many aspects of NSC behavior, such as balancing the quiescent and proliferative status of NSCs (in order to regulate the rate of neurogenesis), determining the cell division mode (symmetric versus asymmetric, to preserve the NSC pool), and preventing premature depletion of stem cells, or the loss of their properties, to maintain neurogenesis throughout life (Morrison and Spradling, 2008; Miller and Gauthier-Fisher, 2009). Disrupted homeostatic influence of neurogenic niches onto NSCs can promote pathological conditions such as cellular aging and tumorigenesis (Voog and Jones, 2010). Thus, identifying and understanding niche signals can shed light on how adult neurogenesis is regulated and can provide a key to successful NSC-mediated regenerative medicine.

Here, we have addressed the function of BMP signaling in the hippocampal stem cell niche from fully mature mice by combining in vitro experiments, brain infusion of the antagonist Noggin, label-retaining assays, and conditional inactivation of *Bmpr1a* or *Smad4* in stem cells. On the basis of our findings, we propose that BMPs participate as dominant niche signals in the adult hippocampus to restrict proliferation of the stem cell pool. All our studies supported this notion, demonstrating that (1) BMP canonical signaling is active in the majority of the SOX2$^+$ cell population in the hippocampus, which is predominantly out of the cell cycle (Suh et al., 2007), including the BMPRI-A$^+$ radial stem cell pool; (2) BMP canonical signaling is blocked in SOX2$^+$ cells that actively proliferate and incorporate BrdU; (3) BMPs reversibly counteract the mitogenic stimulation of cultured SOX2$^+$ AH-NSCs, driving the cells into quiescence; and (4) downregulation of endogenous BMP signaling increases proliferation of SOX2$^+$ cells in the hippocampus by recruiting quiescent (G_0) radial cells into the cycle and consequently leads to enhanced neurogenesis. Thus, the ultimate role of BMPs in the adult hippocampal niche is to govern the balance between the quiescent and proliferative state of NSCs, thereby modulating stem cell activity and neurogenesis in the SGZ. These results consolidate BMP ligands and BMPR-IA signaling as widespread regulators of stem cell division in a variety of adult somatic niches (Varga and Wrana, 2005; Morrison and Spradling, 2008). In addition, we have also found that canonical signaling becomes reactivated in the hippocampus shortly after neuronal fate commitment, possibly implicating the BMPR-IB receptor in the maturation and/or cell cycle exit of newly born neurons (Figure S7).

Our studies also provided a mechanistic understanding of how BMPs transduce signals into NSCs. BMPR-IA is responsible for triggering the canonical BMP pathway by phosphorylating the SMAD1 protein. Using both adherent and neurosphere stem cell cultures, we have found that the canonical BMP pathway primarily acts to restrict AH-NSC division in the presence of a mitogenic stimulus without affecting stem cell identity. The decrease in proliferation is due, at least in part, to an increase in the proportion of cells that enters quiescence. The effect is reversible and proliferation is resumed once the culture is depleted of BMP. Moreover, translocation of P-SMAD1 is associated with the upregulation of target genes, such as *Id1-4* and *Hes1*. All the aforementioned genes are known to block the action of prodifferentiation bHLH factors in the developing ventricular zone of the central nervous system (Ishibashi et al., 1994; Nakashima et al., 2001; Ohtsuka et al., 2001; Hatakeyama

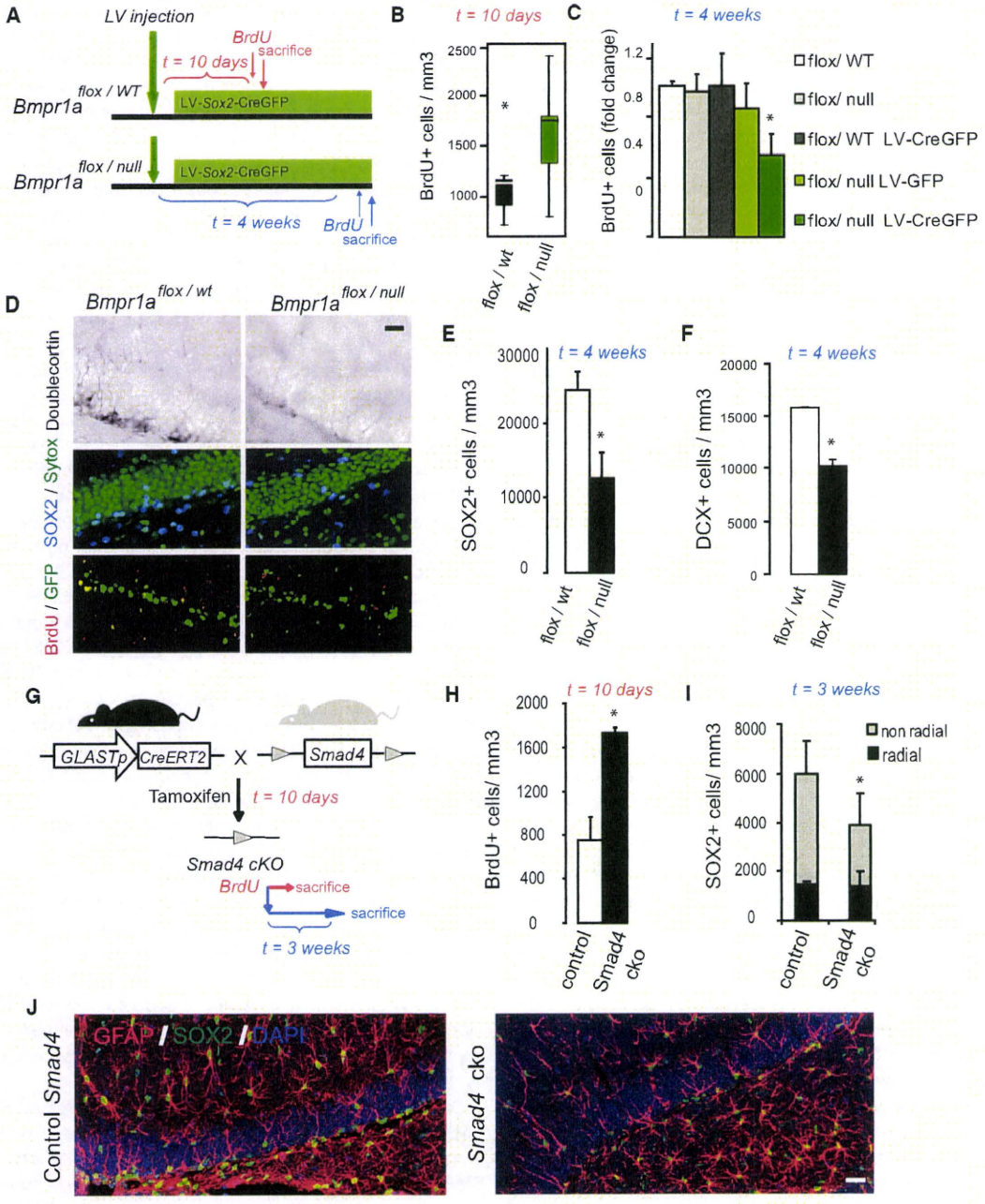

Figure 7. Conditional Ablation of *Bmpr1a* or *Smad4* Compromises Stem Cell Maintenance and Neurogenesis

(A) Scheme illustrating the LV-based strategy for selective deletion of the *Bmpr1a* allele in *Sox2*-expressing cells. BrdU was administered prior to sacrifice, either 10 days or 4 weeks after LV injection.

(B) Box and whiskers plot showing that median proliferation is increased in $Bmpr1a^{flox/null}$ mice injected with the LV expressing GFP/Cre fusion in $SOX2^+$ cells after 10 days. Note the dispersion of the data at this early time point (Mann-Whitney U-test, $p < 0.05$).

(C) Proliferation is significantly decreased in $Bmpr1a^{flox/null}$ mice injected with the LV expressing GFP/Cre after 4 weeks. No change was observed in noninjected contralateral hemispheres (control) or in $Bmpr1a^{flox/null}$ mice injected with the LV expressing GFP.

(D) Immunohistochemical analysis of $Bmpr1a^{flox/null}$ and $Bmpr1a^{flox/wt}$ mice injected with the LV expressing GFP/Cre after 4 weeks. The number of proliferating cells (bottom, $BrdU^+$, red), the number of stem/precursor cells (middle, $SOX2^+$, blue), and the number of new neurons (top, DCX^+, gray) were reduced. SGZ LV-infected cells expressing GFP (green) are shown in the bottom panel.

(E) Quantitative analysis of $Bmpr1a^{flox/null}$ and $Bmpr1a^{flox/wt}$ mice injected with the LV expressing GFP/Cre demonstrates the depletion in $SOX2^+$ cells.

(F) The reduction in the number of DCX^+ neurons observed in (D).

et al., 2004). Induction of the *Hes1* gene is particularly interesting because HES1 can act as a safeguard against irreversible cell cycle exit during quiescence, thereby possibly preventing premature senescence and inappropriate differentiation of AH-NSCs (Sang et al., 2008). As opposed to the BMP treatment, the addition of the antagonist Noggin to neurosphere cultures increased the number of spheres, their diameter, and the percentage of cells per sphere that were in the cell cycle, indicating that AH-NSCs secrete BMPs, which may act to regulate proliferation in an autocrine manner.

A relevant aspect of our in vivo results is that although blockade of BMP signaling in the hippocampus first stimulates proliferation, it leads subsequently to the loss of the regenerative capacity of the radial stem cell population. The early impact of Noggin infusion is an increase in proliferation, but the consequence after 3 weeks is a reduction in proliferation and a depletion of newborn neurons (which were also detected in *Smad4*- and *Bmpr1a*-deleted animals). Importantly, by consecutively labeling cells with CldU and IdU, we observed that $CldU^+IdU^+$ double-positive cells in the SGZ were diminished 4 weeks after the onset of Noggin infusion, pointing to a restriction in the proliferative activity of the LRCs that were challenged to divide earlier. This finding differs from a recent report showing that continuous Noggin release from neuronal cells increases the number of slowly dividing LRCs (Bonaguidi et al., 2008). However, in that study, the interval between the administration of the two thymidine analogs was shorter, perhaps explaining their different results. Alternatively, it is possible that acute delivery of Noggin by pump infusion may have caused a response that differs from the effect triggered by a continuous Noggin release. Interestingly, we also observed that 4 weeks after blocking the BMP pathway, the number of nonradial $SOX2^+$ cells was reduced, whereas the number of $SOX2^+$ $GFAP^+$ radial cells remained constant. This observation is compatible with a model in which the production of nonradial cells by adult hippocampal radial NSCs in vivo becomes compromised after a certain number of mitotic rounds, resembling the behavior of NSCs in the aged hippocampus (Hattiangady and Shetty, 2008; Aizawa et al., 2009). In conclusion, our interpretation of the data presented herein is that a prolonged blockade of the BMP pathway can lead to a premature loss in the ability of activated hippocampal stem cells to proliferate and generate progeny in vivo. However, at later time points, feedback mechanisms elicited by the decline in stem cell activity could recruit a backup of dormant NSCs to replenish the niche.

Together, our findings reveal an aspect of BMP signaling in adult NSC niches, as a master regulator of quiescence, and may provide a key to understanding the maintenance of neurogenesis in the adult hippocampus. At the same time, our studies raise several questions regarding BMP function. First, it is tempting to speculate that the effects of diverse neurogenic external stimuli, such as learning, voluntary exercise, enriched environment, or treatment with antidepressant drugs (reviewed by Ming and Song, 2005; Zhao et al., 2008), may converge mechanistically on an increase in inhibitory factors that block BMP signaling. In support of this view, it has been reported that running increases *Noggin* expression and decreases *Bmp4* expression in hippocampal tissue, and the resulting blockade of BMP signaling is crucial for the effects of exercise on neurogenesis and cognition in mice (Gobeske et al., 2009). In contrast, it has been shown that decreased neurogenesis in a transgenic mouse model of Alzheimer's disease is accompanied by increased expression of *Bmp4* and decreased expression of *Noggin* (Tang et al., 2009), pointing to a broad role for the niche's balance of BMP antagonists/ligands in controlling adult NSCs. However, the identification of the cellular source of BMP ligands and antagonists in vivo needs to be investigated further. Second, as shown in our in vitro studies, BMPs counteract mitogenic signals such as FGF2; thus, understanding the interplay between the BMP pathway and other signaling pathways may be crucial to unraveling how adult NSC division is balanced. Among the endogenous molecules that are expressed in the dentate gyrus of rodents and that have been shown to regulate hippocampal NSCs, Shh (Favaro et al., 2009) and Wnt3 (Lie et al., 2005) may be relevant (Figure S7). Given the antagonistic function of BMP and Shh in mediating the development of some central nervous system structures, and given the role of the fine-tuned activity of the BMP and Wnt pathways in the switch from stem cell quiescence to active proliferation in several adult organs (reviewed by Li and Clevers, 2010), future attempts should be made to understand the function of BMP signaling in a context-dependent manner.

EXPERIMENTAL PROCEDURES

Cell Culture

For proliferation and electroporation assays, AH-NSCs were grown as described in Supplemental Experimental Procedures. Recombinant BMP2/BMP4 (R&D Systems) and Noggin (Sigma) were added at the indicated concentrations.

Immunostaining

Tissue and cultured cells were fixed with 4% paraformaldehyde and processed for immunostaining. Primary and secondary antibodies employed are listed in Supplemental Experimental Procedures. Stained specimens were analyzed with either a Bio-Rad Radiance confocal imaging system (Hercules, CA), a Leica TCS-SL spectral confocal (Heidelberg, Germany), or a Nikon Eclipse 800 microscope (Nikon, Melville, NY).

Flow Cytometry

Analysis was performed on Hoechst 33342 (Sigma) and Pyronin Y (Sigma) stained cells with a FACSVantage cytometer (Becton Dickinson), as described in Supplemental Experimental Procedures. Oregon Green 488 carboxylic acid diacetate succimidyl ester (DFFDA, Molecular Probes) was used for staining neurospheres. $DFFDA^{high}$ cells were sorted in FACSAria (Becton Dickinson) equipment.

(G) Diagram illustrating the experimental design employed for the selective deletion of *Smad4* in GLAST-expressing adult radial stem cells. BrdU was injected 10 days after the administration of tamoxifen. Animals were either sacrificed immediately after or 3 weeks later.
(H) Soon after tamoxifen treatment, proliferation in the SGZ of *Smad4* conditional knockouts was increased.
(I and J) Three weeks later, the number of nonradial precursors diminished but the number of radial NSCs remained unchanged. The confocal image shows the maximal projection of a 17-micron stack. GFAP staining is shown in red, SOX2 is shown in green, and DAPI is shown in blue. Unpaired Student's t test: $^*p < 0.05$. The scale bar represents 40 μm.

Intracerebroventricular Infusion

Infusion was performed using Alzet osmotic mini-pumps (see Supplemental Experimental Procedures for additional details). In one experimental paradigm, animals were injected intraperitoneally with 50 mg BrdU/kg of body weight (seven times, once every 2 hours) on the last day of infusion and were sacrificed 1 hr after the last injection. In a second experimental paradigm, CldU (42.5 mg/kg) was injected on the last day of infusion (three times every 2 hr). Next, the catheter connecting the pump to the cannula was sealed. After 3 additional weeks, animals received IdU (57.5 mg/kg) over 3 days (six times every 12 hr) and were sacrificed 12 hr after the last injection. Handling of mice was carried out in accordance with 86/609/EEC guidelines. The animal procedures were performed in accordance with protocols approved by the Instituto de Salud Carlos III animal care and use committee.

Lentiviral Vectors and In Vivo Injections

Lentiviral vectors expressed either GFP or GFP/Cre fusion protein under the control of *Sox2* promoter. A total of 1.5 µl of the viral concentrate was stereotactically injected into the right hippocampal dentate gyrus (see Supplemental Experimental Procedures for additional details). Ten days post-surgery, animals were injected intraperitoneally with BrdU four times at 2 hr intervals and were sacrificed two hours after the last injection. A separate group of animals was injected with BrdU four weeks post-surgery, once daily for three consecutive days, at a dose of 100 mg/kg body weight. Animals were perfused 24 hr after the final BrdU injection. All animal procedures were performed according to protocols approved by The Salk Institute for Biological Studies animal care and use committee.

SUPPLEMENTAL INFORMATION

Supplemental Information includes Supplemental Experimental Procedures and seven figures and can be found with this article online at doi:10.1016/j.stem.2010.04.016.

ACKNOWLEDGMENTS

The authors thank Dr.Yuji Mishina for *Bmpr1a*$^{flox/flox}$ and *Bmpr1a*$^{wt/null}$ mice and Dr. C.X. Deng for the *Smad4*$^{flox/flox}$ mice. They also thank Mary Lynn Gage for editorial support, Dr. Pilar Sánchez-Gómez for helpful discussions and suggestions, Dr. Mari Paz Rubio, Maria José Palop, André Luis Carvalho, Mireia Moreno, Yolanda Noriega, and Mario Alía for technical assistance. S.J. was supported in part by the Deutsche Forschungsgemeinschaft; H.M. was supported by the Programa Ramon y Cajal from the Spanish Ministerio de Educacion y Ciencia (MEC); Z.A. was supported by the Centro de Investigación Príncipe Felipe; and M.A.M-T. is a recipient of a pre-doctoral fellowship from the FPI/MEC. M.G. was funded by Helma and SFB 596. Additional support was provided by grants from Ministerio de Sanidad y Consumo (MSC; Fondo de Investigación Sanitaria-PI06/0754 and PI09/2254) to H.M.; from MEC (SAF2005-06325), MSC (RETIC Tercel and CIBERNED) and Fundación "la Caixa" to I.F., and from the Bavarian Network on Adult Neural Stem Cells "FORNEUROCELL" to D.C.L.

Received: October 3, 2008
Revised: November 13, 2009
Accepted: April 13, 2010
Published: July 1, 2010

REFERENCES

Aizawa, K., Ageyama, N., Terao, K., and Hisatsune, T. (2009). Primate-specific alterations in neural stem/progenitor cells in the aged hippocampus. Neurobiol. Aging, in press. Published online February 6, 2009. 10.1016/j.neurobiolaging.2008.12.011.

Bonaguidi, M.A., Peng, C.Y., McGuire, T., Falciglia, G., Gobeske, K.T., Czeisler, C., and Kessler, J.A. (2008). Noggin expands neural stem cells in the adult hippocampus. J. Neurosci. *28*, 9194–9204.

Charytoniuk, D.A., Traiffort, E., Pinard, E., Issertial, O., Seylaz, J., and Ruat, M. (2000). Distribution of bone morphogenetic protein and bone morphogenetic protein receptor transcripts in the rodent nervous system and up-regulation of bone morphogenetic protein receptor type II in hippocampal dentate gyrus in a rat model of global cerebral ischemia. Neuroscience *100*, 33–43.

Chen, H.L., and Panchision, D.M. (2007). Concise review: Bone morphogenetic protein pleiotropism in neural stem cells and their derivatives—alternative pathways, convergent signals. Stem Cells *25*, 63–68.

Cheng, T., Rodrigues, N., Shen, H., Yang, Y., Dombkowski, D., Sykes, M., and Scadden, D.T. (2000). Hematopoietic stem cell quiescence maintained by p21cip1/waf1. Science *287*, 1804–1808.

Colak, D., Mori, T., Brill, M.S., Pfeifer, A., Falk, S., Deng, C., Monteiro, R., Mummery, C., Sommer, L., and Götz, M. (2008). Adult neurogenesis requires Smad4-mediated bone morphogenic protein signaling in stem cells. J. Neurosci. *28*, 434–446.

Coskun, V., Venkatraman, G., Yang, H., Rao, M.S., and Luskin, M.B. (2001). Retroviral manipulation of the expression of bone morphogenetic protein receptor Ia by SVZa progenitor cells leads to changes in their p19(INK4d) expression but not in their neuronal commitment. Int. J. Dev. Neurosci. *19*, 219–227.

Favaro, R., Valotta, M., Ferri, A.L., Latorre, E., Mariani, J., Giachino, C., Lancini, C., Tosetti, V., Ottolenghi, S., Taylor, V., and Nicolis, S.K. (2009). Hippocampal development and neural stem cell maintenance require Sox2-dependent regulation of Shh. Nat. Neurosci. *12*, 1248–1256.

Filippov, V., Kronenberg, G., Pivneva, T., Reuter, K., Steiner, B., Wang, L.P., Yamaguchi, M., Kettenmann, H., and Kempermann, G. (2003). Subpopulation of nestin-expressing progenitor cells in the adult murine hippocampus shows electrophysiological and morphological characteristics of astrocytes. Mol. Cell. Neurosci. *23*, 373–382.

Fukuda, S., Kato, F., Tozuka, Y., Yamaguchi, M., Miyamoto, Y., and Hisatsune, T. (2003). Two distinct subpopulations of nestin-positive cells in adult mouse dentate gyrus. J. Neurosci. *23*, 9357–9366.

Gobeske, K.T., Das, S., Bonaguidi, M.A., Weiss, C., Radulovic, J., Disterhoft, J.F., and Kessler, J.A. (2009). BMP signaling mediates effects of exercise on hippocampal neurogenesis and cognition in mice. PLoS ONE *4*, e7506.

Hall, A.K., and Miller, R.H. (2004). Emerging roles for bone morphogenetic proteins in central nervous system glial biology. J. Neurosci. Res. *76*, 1–8.

Hatakeyama, J., Bessho, Y., Katoh, K., Ookawara, S., Fujioka, M., Guillemot, F., and Kageyama, R. (2004). Hes genes regulate size, shape and histogenesis of the nervous system by control of the timing of neural stem cell differentiation. Development *131*, 5539–5550.

Hattiangady, B., and Shetty, A.K. (2008). Aging does not alter the number or phenotype of putative stem/progenitor cells in the neurogenic region of the hippocampus. Neurobiol. Aging *29*, 129–147.

Ishibashi, M., Moriyoshi, K., Sasai, Y., Shiota, K., Nakanishi, S., and Kageyama, R. (1994). Persistent expression of helix-loop-helix factor HES-1 prevents mammalian neural differentiation in the central nervous system. EMBO J. *13*, 1799–1805.

Kippin, T.E., Martens, D.J., and van der Kooy, D. (2005). p21 loss compromises the relative quiescence of forebrain stem cell proliferation leading to exhaustion of their proliferation capacity. Genes Dev. *19*, 756–767.

Kronenberg, G., Reuter, K., Steiner, B., Brandt, M.D., Jessberger, S., Yamaguchi, M., and Kempermann, G. (2003). Subpopulations of proliferating cells of the adult hippocampus respond differently to physiologic neurogenic stimuli. J. Comp. Neurol. *467*, 455–463.

Li, L., and Clevers, H. (2010). Coexistence of quiescent and active adult stem cells in mammals. Science *327*, 542–545.

Lie, D.C., Colamarino, S.A., Song, H.J., Désiré, L., Mira, H., Consiglio, A., Lein, E.S., Jessberger, S., Lansford, H., Dearie, A.R., and Gage, F.H. (2005). Wnt signalling regulates adult hippocampal neurogenesis. Nature *437*, 1370–1375.

Lim, D.A., Tramontin, A.D., Trevejo, J.M., Herrera, D.G., García-Verdugo, J.M., and Alvarez-Buylla, A. (2000). Noggin antagonizes BMP signaling to create a niche for adult neurogenesis. Neuron *28*, 713–726.

Miller, F.D., and Gauthier-Fisher, A. (2009). Home at last: Neural stem cell niches defined. Cell Stem Cell *4*, 507–510.